RI 8896

Bureau of Mines Report of Investigations/1984

Effects of Repeated Blasting on a Wood-Frame House

By Mark S. Stagg, David E. Siskind,
Michael G. Stevens, and Charles H. Dowding

UNITED STATES DEPARTMENT OF THE INTERIOR

112.7

Report of Investigations 8896

Effects of Repeated Blasting on a Wood-Frame House

By Mark S. Stagg, David E. Siskind,
Michael G. Stevens, and Charles H. Dowding

UNITED STATES DEPARTMENT OF THE INTERIOR
William P. Clark, Secretary

BUREAU OF MINES
Robert C. Horton, Director

Library of Congress Cataloging in Publication Data:

Effects of repeated blasting on a wood-frame house.

(Report of investigations ; 8896)

Bibliography: p. 55-59.

Supt. of Docs. no.: I 28.23:8896.

1. Earth movements and building. 2. Blast effect. 3. Structural dynamics. I. Stagg, Mark S. II. Series: Report of investigations (United States. Bureau of Mines) ; 8896.

TN23.U43 [TH1094] 622s [690'.21] 84-7651

CONTENTS

ILLUSTRATIONS

ILLUSTRATIONS--Continued

ILLUSTRATIONS--Continued

TABLES

UNIT OF MEASURE ABBREVIATIONS USED IN THIS REPORT

°C	degree Celsius	kg	kilogram
dB	decibel	kgf•m	kilogram (force) meter
°F	degree Fahrenheit	kHz	kilohertz
ft	foot	kW	kilowatt
ft^2	square foot	m	meter
$ft/lb^{1/2}$	foot per square-root pound (scaled distance)	mi	mile
		mi/h	mile per hour
ft/s^2	foot per square second	min	minute
G	gravity (32.2 ft/s^2)	µin/in	microinch per inch
h	hour	mm	millimeter
Hz	hertz	mm/°C	millimeter per degree Celsius
hp	horsepower	mm/s	millimeter per second
in	inch	N	Newton
in/min	inch per minute	N/mm^2	Newton per square millimeter
in/s	inch per second	pct	percent
lb	pound	s	second
lbf	pound (force)	V	volt
lbf/ft^2	pound (force) per square foot	V/mm	volt per millimeter
lbf/in^2	pound (force) per square inch	yr	year
lbf/in	pound (force) per inch		

EFFECTS OF REPEATED BLASTING ON A WOOD-FRAME HOUSE

By Mark S. Stagg,[1] David E. Siskind,[2] Michael G. Stevens,[3] and Charles H. Dowding[4]

ABSTRACT

The Bureau of Mines arranged to have a wood-frame test house built in the path of an advancing surface coal mine so it could investigate the effects of repeated blasting on a residential house. Structural fatigue and damage were assessed over a 2-yr period. The house was subjected to vibrations from 587 production blasts with particle velocities that varied from 0.10 to 6.94 in/s. Later, the entire house was shaken mechanically to produce fatigue cracking. Failure strain characteristics of construction materials were evaluated as a basis for comparing strains induced by blasting and shaker loading to those induced by weather and household activities.

Cosmetic or hairline cracks 0.01 to 0.10 mm wide occurred during construction of the house and also during periods when no blasts were detonated. The formation of cosmetic cracks increased from 0.3 to 1.0 cracks per week when ground motions exceeded 1.0 in/s. Human activity and changes in temperature and humidity caused strains in walls that were equivalent to those produced by ground motions up to 1.2 in/s. When the entire structure was mechanically shaken, the first crack appeared after 56,000 cycles, the equivalent of 28 yr of shaking by blast-generated ground motions of 0.5 in/s twice a day.

[1]Civil engineer, Twin Cities Research Center, Bureau of Mines, Minneapolis, MN.
[2]Supervisory geophysicist, Twin Cities Research Center.
[3]Mining engineer, Twin Cities Research Center (now with Bureau of Land Reclamation, U.S. Department of the Interior, Denver, CO).
[4]Associate professor of civil engineering, Northwestern University, Evanston, IL.

INTRODUCTION

Ground vibrations from surface mine blasting can be a serious problem for the mining industry, governmental agencies responsible for regulating their adverse environmental effects, and the public which is subjected to them. The Bureau of Mines recently completed two major studies which determined the ground vibration and airblast levels that correspond to structural vibration response and cracking of interior walls (1-2).[5] These studies established levels for both airblast and ground vibrations above which the probability of blast-produced damage increases. They included a study of 58 residences and 9 other related blasting studies. They were, by design, short term studies at relatively high vibration values.

The cracks observed in these previous studies were primarily extensions or inceptions of cosmetic cracks (0.01 to 0.1 mm wide) in older plaster walls. However, the initial building distortion and preexisting wall strains were unknown, and little could be learned about fatigue effects from repeated blasts. In addition, these studies demonstrated that even when a peak vibration criterion is not exceeded, complaints are still possible and often are accompanied by claims of damage attributed to fatigue.

Several authors have postulated that repeated low-level vibrations accelerate the normal cracking process caused by environmental factors such as age, settlement, wind, temperature, humidity, and human activities (3-6). Research results on fatigue and failure of materials used in residential construction have been limited and inconsistent (2, 4-10). They do, however, suggest that fatigue effects are possible both from vibrations and natural causes (7-10).

To assess (1) the fatigue behavior of structural materials when repeatedly loaded by blast-induced vibrations and (2) the role of naturally occurring stresses, the Bureau conducted a long term field and laboratory study. Researchers studied the vibration and strain response of a typical contractor-built home in the path of an advancing surface coal mine over a 2-yr period. Upon completion of the blasting tests, mechanical shakers were used to simulate an increase in the total number of load cycles well beyond that expected from natural stress-inducing phenomena and blasting to ensure a complete fatigue assessment.

Bureau researchers also conducted a parallel laboratory program to obtain basic failure properties of wallboard and masonry walls. The failure characteristics of wallboard in shear, tension, and bending and of wallboard paper in tension were evaluated. These analyses provided the basis for using strain readings to assess the relative impact of blast-induced stresses to those of human activities and naturally occurring stresses. Through a Bureau contract, the National Bureau of Standards (NBS) performed similar property tests on masonry block walls (11). This report describes both the field and laboratory studies and presents the findings from both.

BACKGROUND

Cracking in structures from repeated blasting vibrations involves many aspects that have been previously studied, such as criteria and construction details to prevent cracking; causes of cracking, including effects of construction, material condition, and building environment and age; and the rate of new cracks from ambient causes. Since cracks are generally unexpected and their acceptance varies with width, location, and extent, the role of human perception has also been investigated.

[5]Underlined numbers in parentheses refer to items in the list of references preceding the appendixes.

ORIGINS OF CRACKS

Current house-building practices address basic human safety. Many of these practices were derived from allowable deflection criteria in which material cracking potential is considered (12-14). In 1948, Whittemore (15) discussed the problem of the lack of guidelines for vibrations of floors and pointed out that "deflection and vibration can be decreased, but only at an increase in price." Crist (16) echoed Whittemore's conclusion in proposing a static criterion based on the risk of cosmetic cracking. He developed a model performance criterion for floors in line with human acceptability (with respect to vibrations) according to the International Standards Organization's (ISO) proposed standard, which has since been updated (17). More recently, weighting factors have been developed for curves from the ISO standard to include effects of the impulsive shock (blast) as perceived in buildings (18).

The detection of cracking is dependent on the type of material covering the walls as well as environmental loads (including vibration). Consequently, it is important to know how the mechanical strength properties of wall coverings influence cracking characteristics. All structures, including residential buildings, are subjected to a variety of stresses which are continually changing. Examples are shrinkage during material curing, annual and daily humidity and temperature expansion and contraction, and frost- and water-induced soil settlement and heave. Deformations also result from human activities (such as jumping, door closings, and walking) and wind gusts; or they may be attributable to vibro-acoustic sources such as blasting, vehicle traffic, aircraft, and internal machinery.

Masonry walls and wallboard under load are usually assessed linearly by a proportional dimension change (strain)[6] until plastic deformation or creep occurs; i.e., the strain increases rapidly, and ultimately the load-carrying capacity or the stress drops to zero. Because most materials tests involve strain measurements, values of strain are typically used to classify materials deformation tolerances, i.e., linear response range. The nonlinear strain response point or initial yield is easily monitored by strain detection systems. Observations of material cracks occur at strain readings beyond the initial yield point primarily due to eye resolution limitations.

The Bureau's laboratory analyses of wallboard and masonry walls, which are detailed in appendix A, showed the following:

For wallboard--

- The gypsum core fails at ~ 350 μin/in in tension and at ~ 1,000 μin/in in bending, based on the nonlinear response points.

- For visual cracking, paper failure is the controlling factor. Its nonlinear response point occurs at ~ 1,000 to 1,200 μin/in (fig. 1). However, visual observation of buckling or cracking is not possible until a slightly higher strain level is reached.

- Strain rate seems to affect ultimate or total failure, but the paper yield point is relatively constant. This allows comparison of various loading factors (e.g., blasting versus other activities and environmental factors).

---

[6] Axial strain is defined as $\Delta\ell/\ell$, where $\Delta\ell$ is the deformation and ℓ is the original length. Axial stress, σ, can be related to strain, ε, by Young's modulus (E): $\sigma = \varepsilon E$.

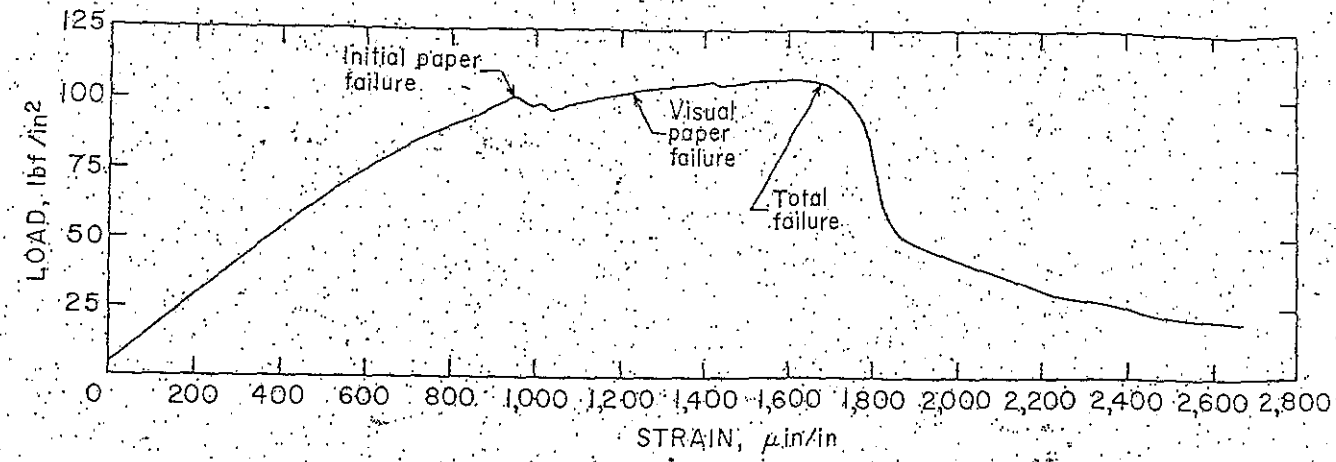

FIGURE 1. - Tensile stress strain-deformation curve for 1/2-in-thick wallboard.

• Once the wallboard cracked, cyclic opening and closing of up to 0.1 mm was observed, and these movements were unaffected by blasting activities.

• Data on cyclic loading behavior of wallboard are limited, but results of tests on wood products indicate that fatigue effects can occur at stress (or strain) levels equivalent to 50 pct of static failure conditions, but over 100,000 cycles are required.

For masonry walls--

• Hairline cracks occur primarily at the mortar-and-block interface.

• Observations of tensile cracks at a strain-monitored site showed that such cracks are first detected at strain levels well above the first nonlinear response point because of naked eye limitations (~ 0.01 to 0.1 mm).

• Use of strain gauge readings to describe crack growth to visual widths and beyond can be misleading since the measured strain is dependent on the strain gauge length. For example, strains read at the threshold of visual cracking using different gauge lengths give a different overall strain reading, as illustrated below.

Based on the equation $\varepsilon = \frac{\Delta \ell}{\ell}$,

$$\frac{0.01 \text{ mm}}{13 \text{ mm}} = 770 \ \mu\text{in/in},$$

but $$\frac{0.01 \text{ mm}}{150 \text{ mm}} = 67.0 \ \mu\text{in/in},$$

where ℓ is the gauge length, and the visible crack width is 0.01 mm. Because strain gauge readings can be misleading, crack growth is properly described in terms of displacements.

• Local site strains across the wall vary considerably from global strains. For inplane shear failure, global strain is measured or calculated across the wall diagonally.

• Two cases of cracking due to inplane shear testing were observed:

1. Limited site-specific cracks that can occur at low global strains. These cracks opened and closed up to the point of maximum load and were difficult to distinguish from existing mortar-block separations caused by workmanship and shrinkage.

2. Cracks that propagated across the wall prior to ultimate failure in a steplike pattern along mortar-block interfaces. The global strain approach appears reasonable for failure assessment, but inplane shear failure was shown to be unlikely for homes because of the high compressive loads required.

Cosmetic cracks result when the blasting vibration-induced strain, ε_d, added to some preexisting strain, ε_p, exceeds the critical strain, ε_c. Various criteria such as peak particle velocity, vector sum velocity, pseudo spectral response velocity, displacement, and integrated energy have been suggested for predicting or estimating the potential for blast-induced cracking in structures. However, these criteria provide only an index of blast-induced strains (ε_d). They cannot be related uniformly to the critical wall strain necessary for development or propagation of existing cracks because they do not explicitly consider existing strains (and the corresponding fatigue strength reduction). Monitoring strain, which directly represents material deformation and thus cracking potential, avoids these problems. However, identifying critical measuring locations and their corresponding prestrains is itself a problem, as mentioned in a previous Bureau report, RI 8507 (2).

Differential foundation settlement, excessive structural loads, and material shrinkage induce strains resulting in random and/or patterned cracking. For analyzing blasting effects, these strain-inducing forces are considered static and the resulting strains are called prestrains. For example, consolidation of foundation soil by the transpiration processes of nearby trees (19) causes differential settlement induced prestrain. The walls of residential structures are always under some strain, although cracking may not be apparent. The cracks commonly seen in old homes are manifestations of such prestrains.

Several references present excellent summaries of the multiple origins of cracks (20-23). Basically, cracks are caused by one or a combination of the following:

1. Differential thermal expansion.

2. Structural overloading.

3. Chemical changes in mortar, bricks, plaster, and stucco.

4. Shrinkage and swelling of wood and wood-paper products.

5. Fatigue and aging of wall coverings.

6. Differential foundation settlement.

Another source of strains and cracking--one not usually considered--is everyday household activities. Early in the testing program described in this report, the response of the test house to typical human activity was compared with the response to blasting. Additional human activity data is also available from Andrews' study (3) of the house diagramed in figure 2. Table 1 shows the Bureau's and Andrews' data on wallboard strains resulting from various human activities. Door slamming produced strains greater than those produced from blasting vibrations up to 0.5 in/s. All the strains shown in table 1 are dynamic strains induced by the specified activities; they do not include any prestrains.

Data on prestrain from changes in normal household relative humidity and temperature are limited to paper. These factors have been shown to generate prestrains of ~ 100 to 200 μin/in in unprotected paper (24-26). For cyclic changes in relative humidity above 65 pct, up to 40 pct paper swelling and shrinkage can occur (26).

RATES OF CRACK OCCURRENCES IN RESIDENTIAL STRUCTURES

Structures crack naturally over time, and this section reports the results of several studies wherein the rates of crack occurrences were measured. Holmberg (27) recently analyzed inspection reports to estimate a crack rate for apartment buildings in Sweden. Two apartment buildings were inspected for cracks three times between 1968 and 1980. The number of observed cracks is plotted as a function of time in figure 3. An average of 12 to 13 new cracks per year occurred for these particular structures.

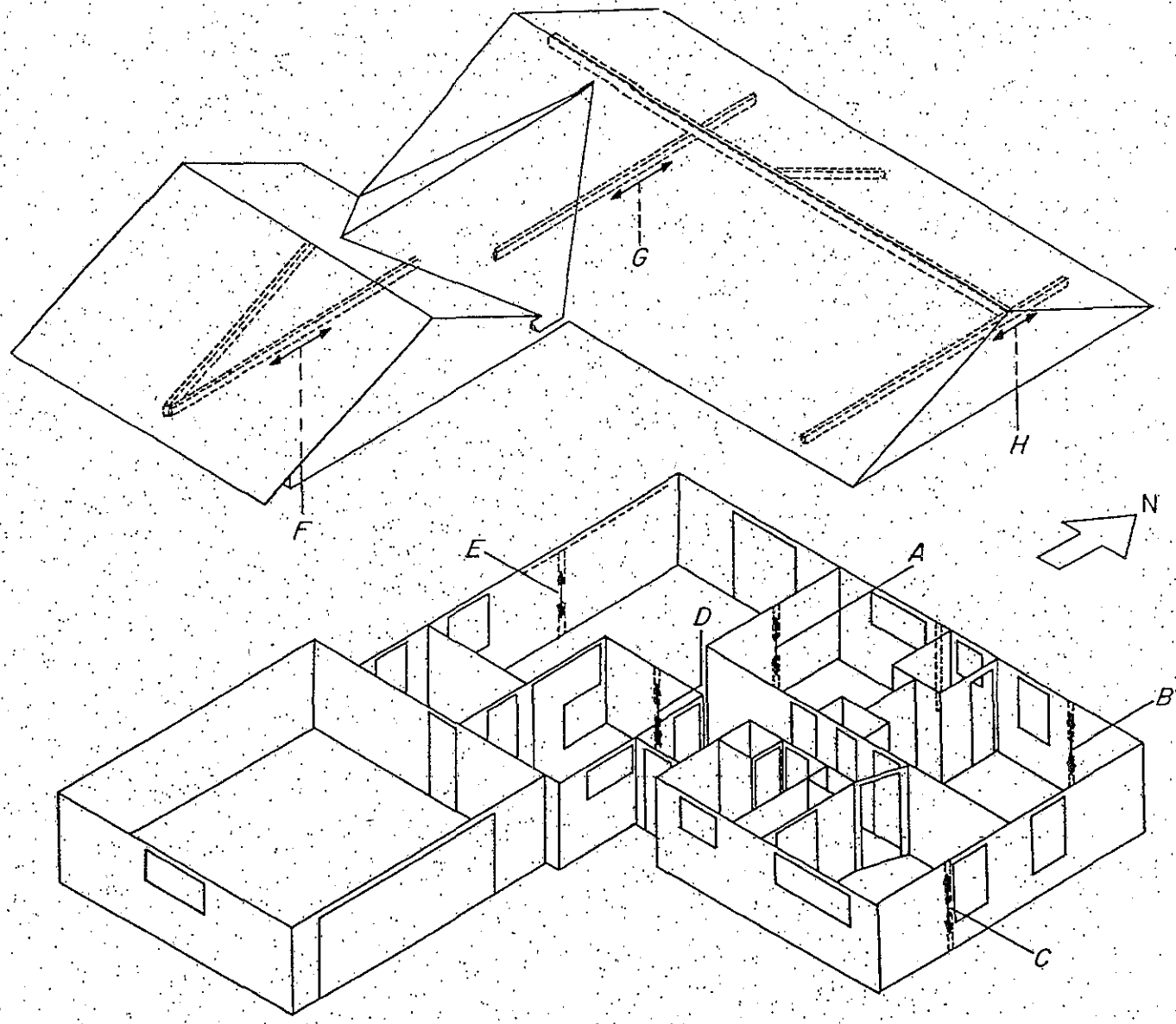

FIGURE 2. - Strain gauge locations in sonic boom study (3), house 1. (Italic letters identify locations listed in table 1.)

TABLE 1. - Maximum strains in wallboard from blasting, household activities, and environmental factors, microinches per inch

Strain location	Mine blasts	Human activities							Wind and/or thunderstorm
		Jumps	Heel drops	Door slams		Nail pounding	Walking		
				Entrance	Sliding glass		1st floor	Attic	
BUREAU OF MINES TEST HOUSE									
Over sliding glass door.	[1]22,[2]15	24	9.2	13	22	21	Low	NM	NM
Over south window in master bedroom.	[3]18	42	20	12	19	9.3	9.1	NM	NM
Over large doorway in living room.	[4]24,[5]11	17	6.1	8.3	6.2	28	Low	NM	NM
Over picture window.	[4]33	17	11	21	3.6	32	3.2	NM	NM
Over entrance door.	[4]36,[5]43	13	5.8	140	Low	Low	Low	NM	NM
ANDREWS' SONIC BOOM STUDY (3), HOUSE 1									
From figure 2, location:									
A	NM	NM	NM	39.1	NM	NM	NM	10.2	2.36
B	NM	NM	NM	17.0	NM	NM	NM	NM	2.18
C	NM	NM	NM	17.1	NM	NM	NM	NM	Low
D	NM	NM	NM	13.4	NM	NM	NM	3.43	3.63
E	NM	NM	NM	11.5	NM	NM	NM	NM	1.11
F	NM	NM	NM	12.5	NM	NM	NM	66.4	2.38
G	NM	NM	NM	NM	NM	NM	NM	59.0	5.15
H	NM	NM	NM	12.5	NM	NM	NM	NM	1.89

NM Not measured.
[1]From peak ground vibration of 0.30 in/s.
[2]From peak ground vibration of 0.21 in/s.
[3]From peak ground vibration of 0.29 in/s.
[4]From peak ground vibration of 0.39 in/s.
[5]From peak ground vibration of 0.32 in/s.

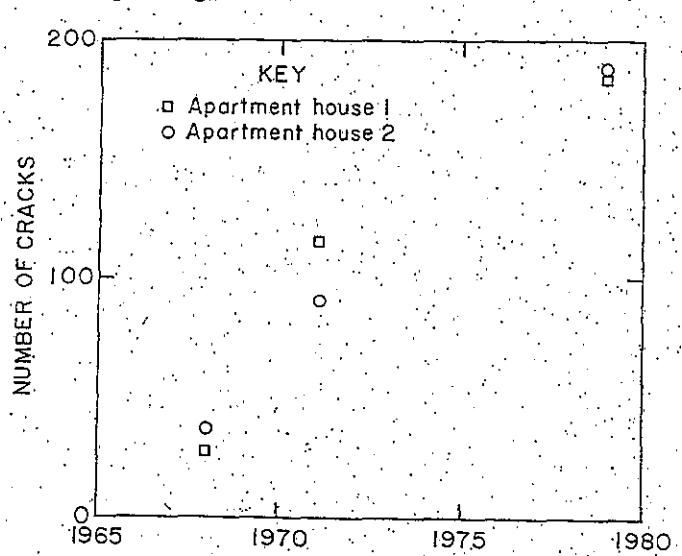

FIGURE 3. - Building age versus crack occurrences, after Holmberg (27).

The crack rate depends upon the type of structure. Rates for 11 wood frame houses that were subjected to 26 weeks of sonic booms and 13 weeks when there were no booms (3) are listed in table 2. Crack rates at homes 1-4, which were studied during both periods, were generally lower during the 13-week nonboom period. The investigators also found evidence of a possible relationship wherein relative humidity and the number of booms may together have an effect on the occurrence of cracks, as shown in figure 4. They concluded, "This investigation has not exonerated sonic booms as a factor influencing the rate of structure deterioration, but neither has it established a direct cause and effect relationship between sonic booms and

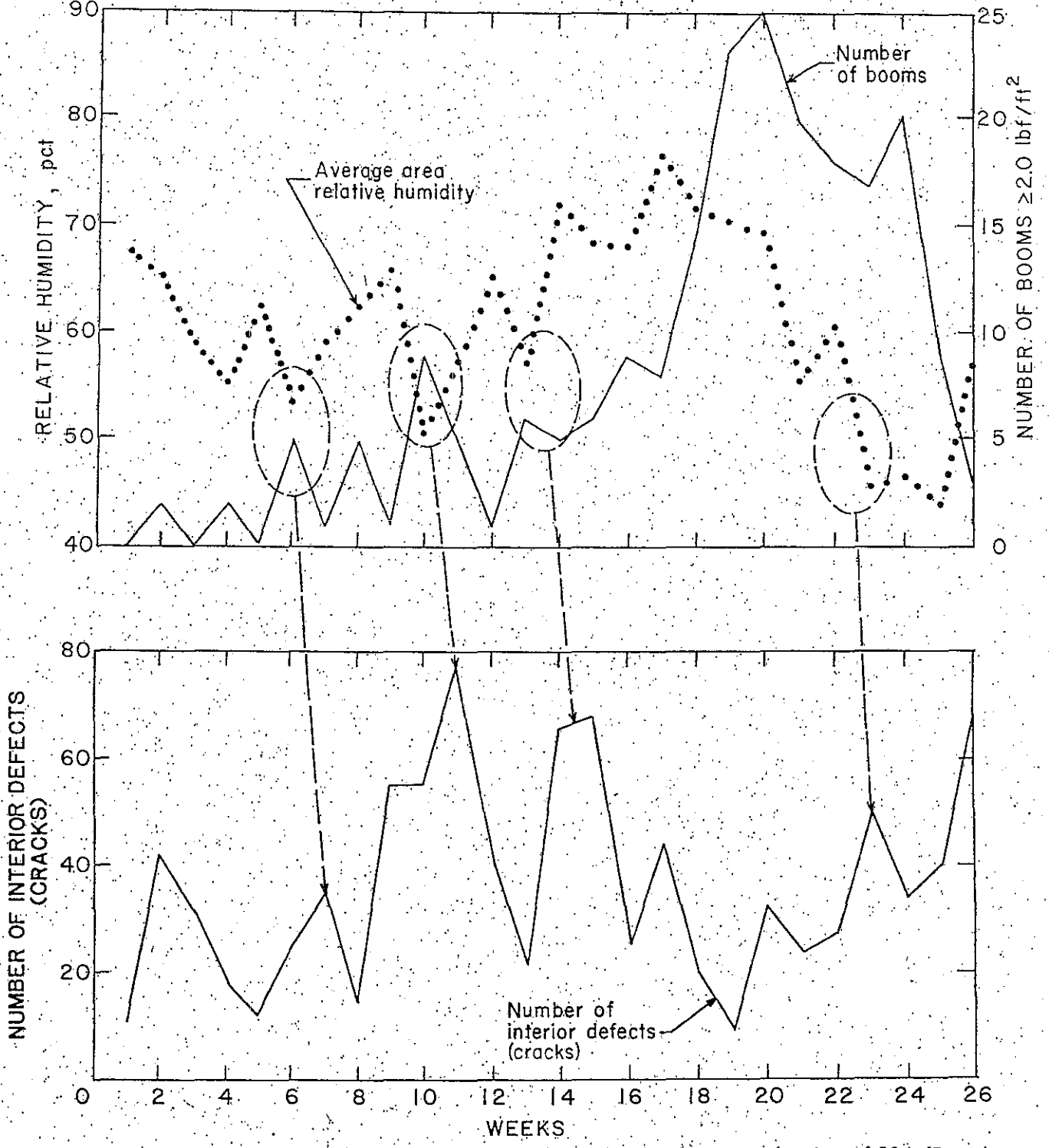

FIGURE 4. - Weekly comparison of crack occurrences to sonic boom amplitudes of 134 dB and to relative humidity (at homes 3 and 4 as shown in table 2).

TABLE 2. - Crack rates for houses subjected to sonic booms (3)

House	Number of stories	Area, ft^2	Foundation	Age, yr	Finish		Occupied	Number of cracks per week	
					Interior	Exterior		Boom period	Nonboom period
1...	1	1,560	Concrete slab.	5	Wallboard..	Brick...	Yes..	3.7	1.9
2...	2	1,750	...do.....	New	...do.....	...do...	No...	8.2	3.3
3...	1	1,470	...do.....	8	...do.....	...do...	No...	8.8	1.5
4...	1	1,160	Concrete stem wall.	18	...do.....	...do...	No...	6.1	1.8
5...	2	2,870	Masonry stem wall.	>50	Plaster and lath.	Asbestos siding.	No...	NM	23
6...	1	1,100	Concrete stem wall.	25	...do.....	Stone...	Yes..	NM	2.6
7...	1	1,090	...do.....	30	Lath and wallboard.	Wood lap	Yes..	NM	1.4
8...	1	1,280	...do.....	30	Plaster and lath.	Brick...	Yes..	NM	3.3
9...	2	2,000	Masonry stem wall.	40	Paper on plaster and lath.	Wood lap	Yes..	NM	3.0
10...	2	2,370	Concrete stem wall.	35	Plaster and lath.	...do...	Yes..	NM	14
11...	1	1,330	Concrete slab.	8	Wallboard..	Brick...	Yes..	NM	2.2

NM Not measured.

defects discovered at the test houses." The crack rates of 1.4 to 23 cracks per week during the nonboom period are quite high compared to the rate observed by Wall (28) in a study of 43 single-story concrete block houses over a 26-week period; he reported a crack rate of 2.5 cracks per day for the 43 houses (<1 crack per week per house).

The large range in the crack rates reported in the separate studies by Holmberg, Andrews (table 2), and Wall is indicative of the wide range of susceptibility of houses to cracking. The rates ranged from near zero to 23 cracks per week. (The cracks-per-year rate reported by Holmberg indicates a cracks-per-week rate of near zero.) None of the investigators reported crack rates of zero. The large differences in the rates reported are partially a result of the difficulty of defining cracks. For example, in Wall's report, shrinkage cracks were ignored, and only new cracks in the moderate (easily distinguishable) range were reported.

These data point out that new cosmetic cracks are likely to occur when months pass between pre- and post-inspections. Therefore, any post-blast inspection is likely to find new cracks that are the result of natural aging. The time frame for inspections and difficulties of observing cracks are discussed in the "Results" section.

ACKNOWLEDGMENTS

The authors acknowledge the cooperation and assistance provided by AMAX Coal Co., Indianapolis, IN, and employees of its Ayrshire Mine (site of the test house) near Evansville, IN, with special thanks expressed to Daniel Lanning, community relations manager; George Martin, general mine manager; Mike Padgett, senior

drilling and shooting supervisor; and John Smith, manager of drilling and shooting. Valuable technical support and advice on strain gauge instrumentation and mechanical problems encountered during this blasting research were provided by Alvin Engler, electrical engineer; Kevin King, electrical engineering student; and G. Robert Vandenbos, electronics technician, employees of the Bureau's Twin Cities Research Center, Minneapolis, MN.

EXPERIMENTAL PROCEDURE

The fatigue research investigation, from June 1979 to December 1981, was based on measurements of structural conditions, dynamic and static responses, and cracking at a full-scale test house located near an operating surface mine. Following the field studies, complementary laboratory tests (appendix A) were performed.

The investigation consisted of the following phases:

1. Design and construction of the test house and installation of monitoring systems for vibration strain, static deformation, and environmental conditions.

2. Long-term monitoring of low strain levels resulting from blasting and other phenomena.

3. High-strain-level blasting as coal mining reached the experimental structure.

4. Extended fatigue loading using mechanical vibrators.

5. Laboratory measurements of the strength and failure characteristics of construction materials.

DESIGN AND CONSTRUCTION OF TEST HOUSE

The experimental plan called for a residential test structure typical of models currently built in the test-site area. The plan also specified the use of common construction materials of the type commonly claimed to have been damaged by blasting. Although plumbing and interior finish work such as inside doors and cupboards were not included, structural integrity required heating and cooling for a realistic home environment.

The Bureau chose a location at the Ayrshire Mine near Evansville, IN, for construction of the test house, and siting of the house there was made possible through an agreement with AMAX Coal Co., the owner of the mine. Figure 5 shows the test-site location and the locations of the blasts relative to the house during the 2-yr test period. The site location allowed a response of at least 1 yr to natural stress-inducing influences before the blast vibrations would reach a level of about 0.75 in/s, the lowest level at which a probability of cracking wallboard had been observed in previous research (2).

After site selection, the Bureau contacted the local carpenters' union to establish the typical house design, then chose a split-level model. The 1,144-ft^2 test house (fig. 6) had a concrete block basement, brick veneer, and a brick fireplace. Interior walls were 1/2-in wallboard with taped and plastered joints. The kitchen-dining room area received an additional 3/16-in coat of veneer plaster. Plumbing, cupboards, finish molding, and interior doors were not installed, but 75 concrete blocks were used to simulate normal household loads. Design details are shown in appendix B. Ed Scheesele & Sons, a local contractor, built the structure between June and October 1979. As a cost-saving measure, the Bureau arranged for a local engineering firm, VME-Nitro Consult, Inc. (VME), to conduct construction inspections at the completion of the following stages: (1) footings--before pouring, (2) foundation, (3) frame and masonry, (4) electrical, and (5) finish.

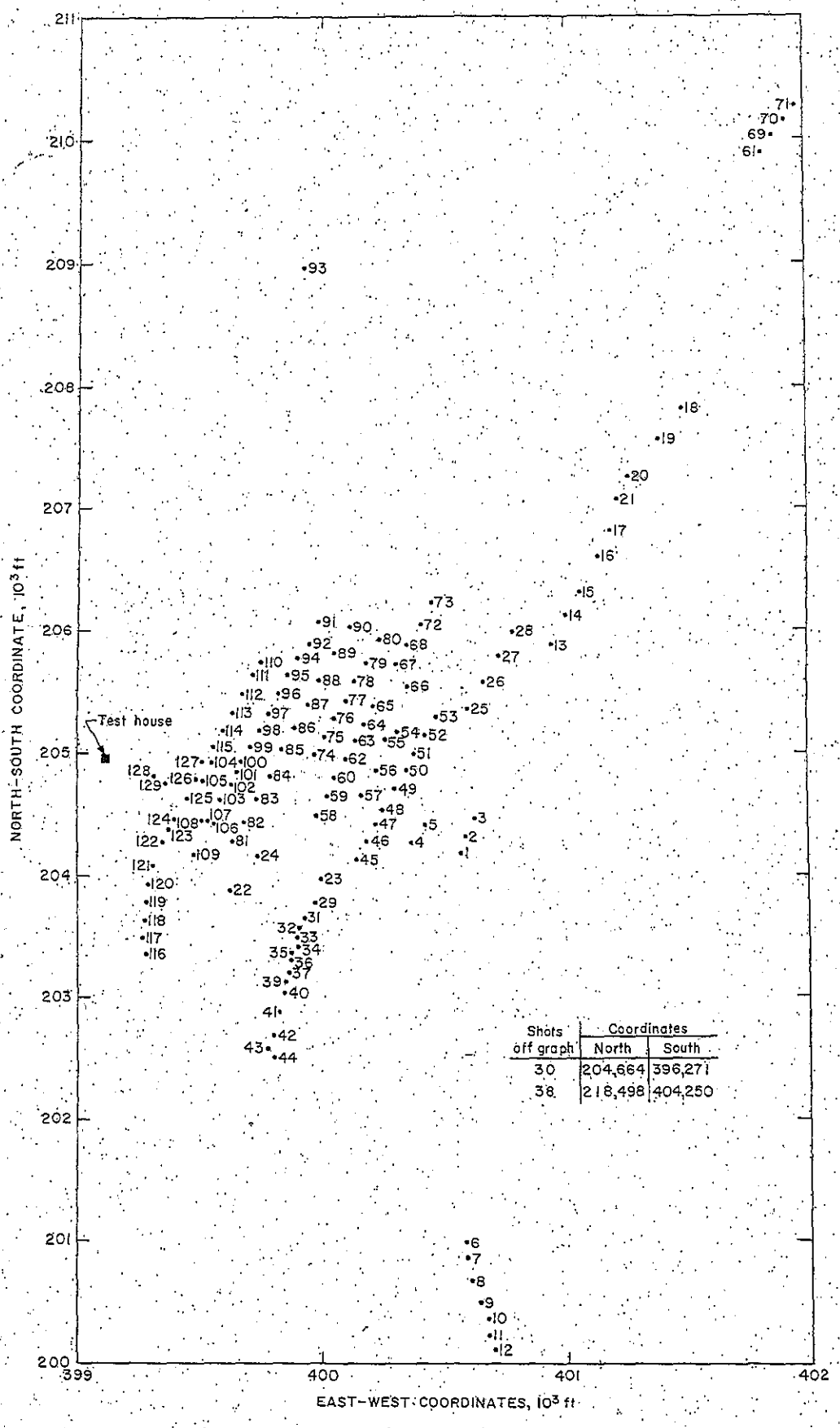

FIGURE 5.- Test house and shot locations.

FIGURE 6. - Front view of test house.

There was one major deviation from the construction plan. The roof framing was changed by the contractor to follow local building practices (fig. B-6). The inspection at construction completion revealed a number of hairline cracks, assumed to be from shrinkage, in wallboard corners and basement block joints.

MONITORING PROGRAM

A multifaceted monitoring program measured the effects of both natural forces and blasting vibrations on the test house. Bureau personnel installed the monitoring instrumentation at the start of the program and operated the systems at critical periods. At other times, VME (under contract) collected the recordings and shipped them to the Bureau's Twin Cities Research Center for processing. Both Bureau and VME personnel were on-site for the final blasts and mechanical fatigue tests, in addition to an engineer from another company, who was responsible for the mechanical vibrator systems.

Low-Level Blasting Tests

During the early phases of the study, static and slowly varying influences were studied. Seasonal weather conditions and effects of settlement and inside environment on static strains and deformations were measured semimonthly at 67 locations within the house. Detailed damage inspections were conducted during the semimonthly testing.

Continuous monitoring of all blasting and weather conditions (both inside and outside environment) was started on October 30, 1979, and continued throughout the study. A Dallas Instruments, Inc., model ST-4 self-triggered seismograph[7] recorded outside vibrations and airblast. Six Rustrak 30-day chart recorders (Gultan Industries, Inc.) monitored temperature, humidity, wind, and, later in the study, two channels of differential displacement (strain). The authors expected that the annual temperature and humidity cycle, as well as daily temperature changes, would introduce cycles of slowly varying stress and consequent strain. They also anticipated that the annual changes (i.e., cross-grain wood shrinkage) would show up in the semimonthly strain measurements. To test for daily variations, a Kaman Sciences Corp. displacement system was used as described later in the "Dynamic Strain" section.

[7]Reference to specific products does not imply endorsement by the Bureau of Mines.

The semimonthly evaluations were made for the Bureau by VME, which was required to do the following for each visit:

1. Perform an elevation survey (transit level loop) of the outside of the test house.

2. Change chart recorder tapes each month for--

Temperature, outside and inside.

Humidity.

Wind speed and direction.

3. Change the ST-4 seismograph tapes.

4. Conduct strain measurements utilizing--

Groove comparitor.

Extensometer.

5. Inspect the structure for cracking; perform mapping and photographing; and note crack lengths and approximate widths.

Periodically during the low-vibration-level phase, dynamic measurements were made of strain and vibration responses, particularly when the mining cycle brought the blasting relatively close to the test house.

The duration of the low-level vibration phase was 16 months, during which the test house was subjected to 645 mining blasts with ground vibrations of <0.75 in/s peak particle velocity. An attempt was made to hold the vibration level of blasts during this period to that level (<0.75 in/s), which is the recommended peak level for Drywall houses (2). Only one shot exceeded this level, by 0.03 in/s, which was within the tolerance of the seismograph's calibration (±10 pct). The house's response to shots 1 to 44 (fig. 5) was recorded during this period.

FIGURE 7. - House relationship to pit (south view).

High-Level Blasting Tests

In March 1981, the mining operation brought the blasting close enough to the house for the vibrations at the test house to exceed 0.75 in/s. Blasting at the working-face area (figs. 7-8) took approximately 1 week to pass by the house during the month-long traverse of the mile-long highwall. During that 1-week period, detailed dynamic measurements and damage inspections were performed. For each blast, strain and vibration time histories were recorded throughout the house (particularly at critical areas near doorways, windows, and corners). At times, as many as 50 FM tape recorder channels were used to record the data.

Structure response and cracking measurements were made periodically over the last 9 months. The house was subjected to approximately 108 blasts >0.5 in/s and one as high as 6.94 in/s. Blasts within 300 to 700 ft and scaled distances of 11 to 30 $ft/lb^{1/2}$ caused the highest ground vibrations.

Mechanical Vibration Tests

The blasting phase of the study ceased when the highwall had reached to within 300 ft of the test house. Although the house had sustained blast-induced cracking by this time, cracking was hairline (except at one corner of the basement) and structural stability had not been affected. Since major damage had not yet occurred, a decision was made to examine fatigue effects by using mechanical shakers to simulate the effects of repeated loading from mine blasts. While results using short-term continuous cyclic loading would probably not be the same as results from long-term repeated loading from mine blasts, they were nonetheless expected to provide an indication of potential fatigue problems. The house had been subjected to as many blasts as are typically received by a structure near an advancing coal mine. However, cases involving long-term (quarry) blasting indicated that further investigation of cyclic loading was warranted.

Two main study options were considered. The first was relocation of the house and continuation of the blasting tests; the second was accelerated fatigue induced by a mechanical shaker. Relocation was considered impractical because of operational constraints that would have been imposed on the mining cycle, costs, and likely additional damage. The main

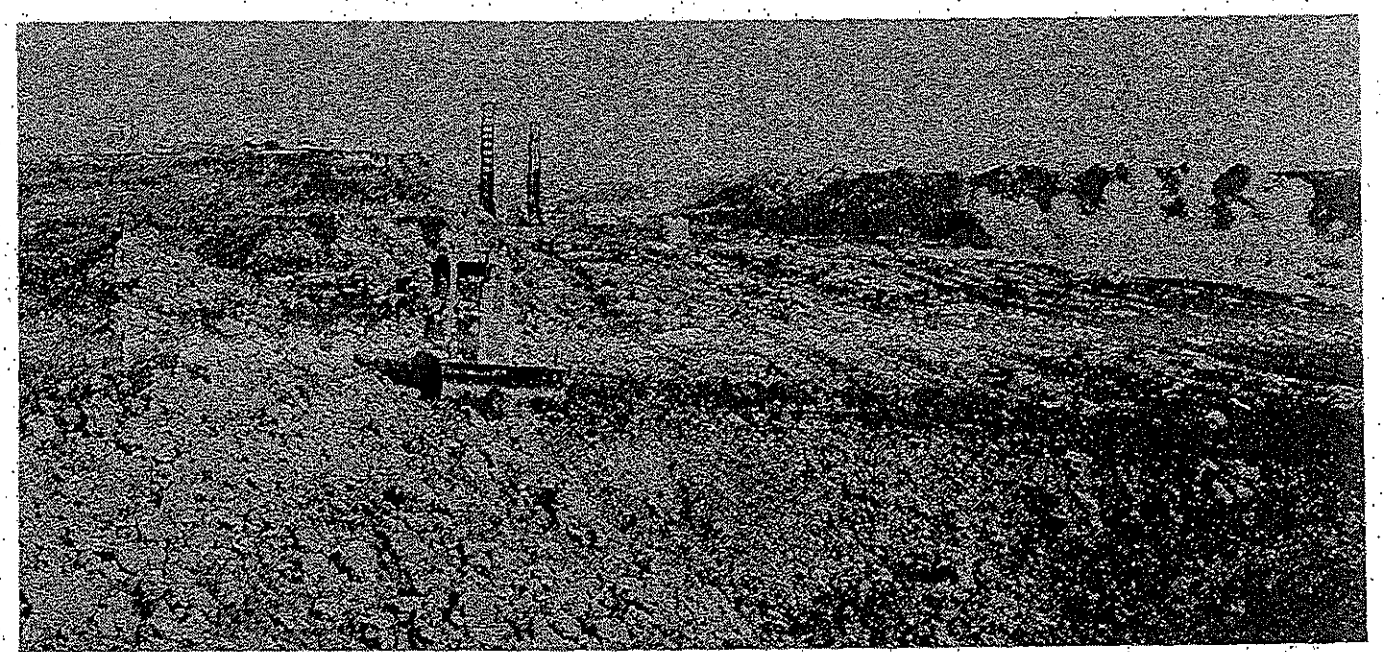

FIGURE 8. - House relationship to pit (north view).

problem with shaker-induced fatigue testing was the time available for testing. There were only two weeks after the final blasting tests in which to set up and conduct the shaker study before the presence of the house would interrupt dragline operations.

An experimental plan had been prepared for the final series of tests, and a contract was let with ANCO Engineers, Inc., to provide and operate the mechanical shaking system. ANCO provided dual-synchronized shakers developed during a previous study of North Sea oil drilling platforms. These shakers were used in the house for accelerated fatigue tests with excitation levels based upon the structure response measured during the blasting tests. Shakers were installed on plywood bolted across the ceiling joists pictured in figure 9, at each end of the test house. Figure 10 shows the installed shaker at the south end of the test house. Table 3 presents the specifications of the shaker system. To avoid stressing the ceiling joists, the shaker weight was transmitted to the foundation by additional column supports (figs. 11 and B-7). In addition, ceiling joist and wall stud connections near the shakers were bolted (fig. 12) to ensure efficient horizontal load transmission during the more than 100,000 loading cycles. The tests involved inducing equivalent structure response until fatigue cracking was observed in the wallboard or until 100,000 cycles was reached at each level of vibration.

Laboratory Failure Tests on Wallboard and Masonry Walls

During the field test program, laboratory support was required in several areas. Special strain-measuring devices were designed, built, tested, and calibrated. Effects of temperature on strain gauges were measured in a cold room. Effects of mounting methods and sensing lengths were also measured. The strain-measuring apparatus and mounting procedures adopted are described in appendix A.

Strength and critical strain levels of wallboard and concrete block walls were also measured in the laboratory to complement the full-scale field tests. The results of these tests and tests by other investigators are reported in appendix A.

TABLE 3. - Mechanical shaker and drive system specifications

Description	2 identical units capable of being driven at speed and in phase to deliver directional sinusoidal forces at 2 different locations.
Operating frequency range	1.5-15.0 Hz.
Frequency control	1.0-0.2 pct over operating range.
Force output, maximum	10,000 lbf (44,500 N) per shaker.
Force range adjustment	0-100 pct of maximum at any given frequency.
Weight including drive motor	1,300 lb (590 kg).
Size	24 by 24 by 24 in (0.6 by 0.6 by 0.6 m).
Drive motors	5.0-hp synchronous induction type, explosionproof.
Electrical requirements:	
Power	7.6 kW.
Voltage	230 V.
Type	3 phase.

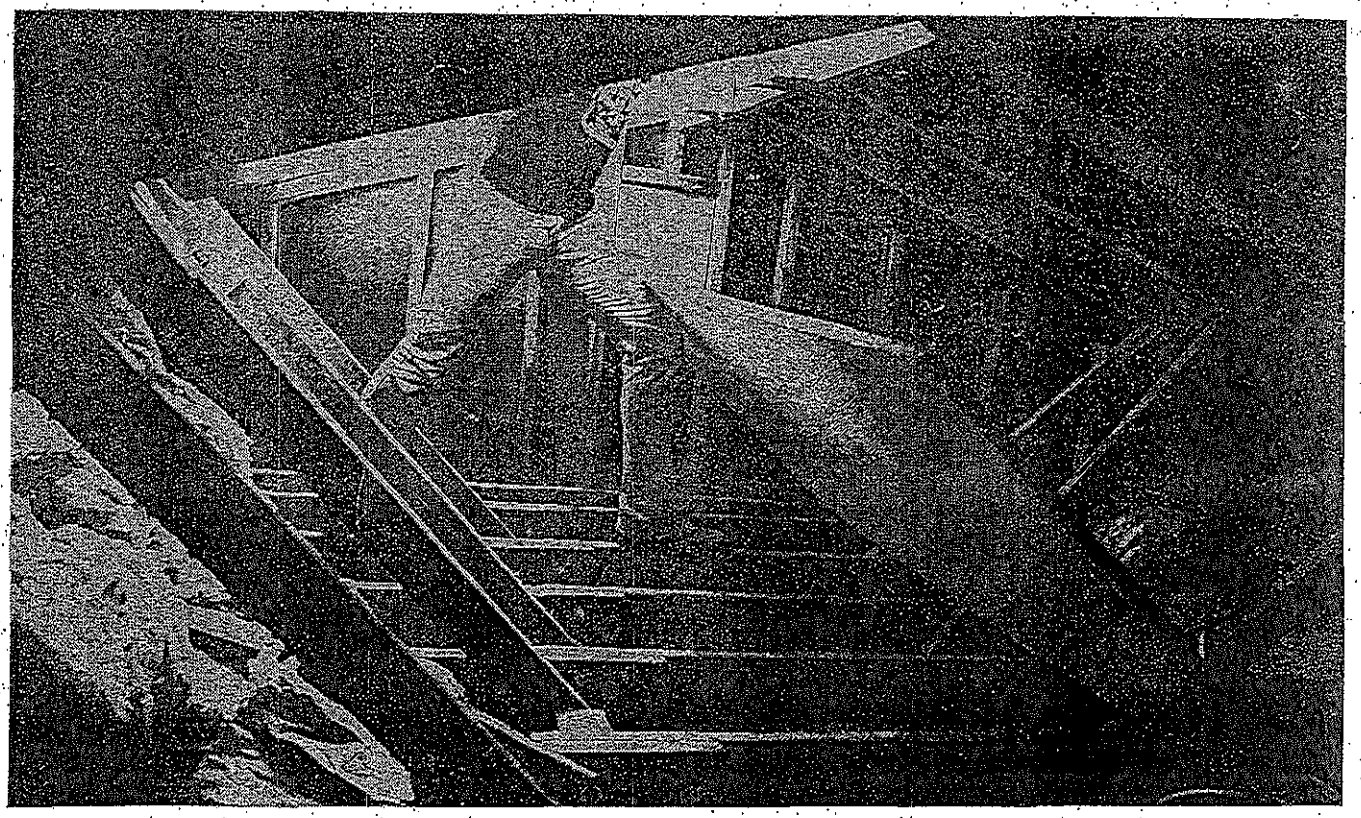

FIGURE 9. - Roof joist preparation for mechanical shaker installation.

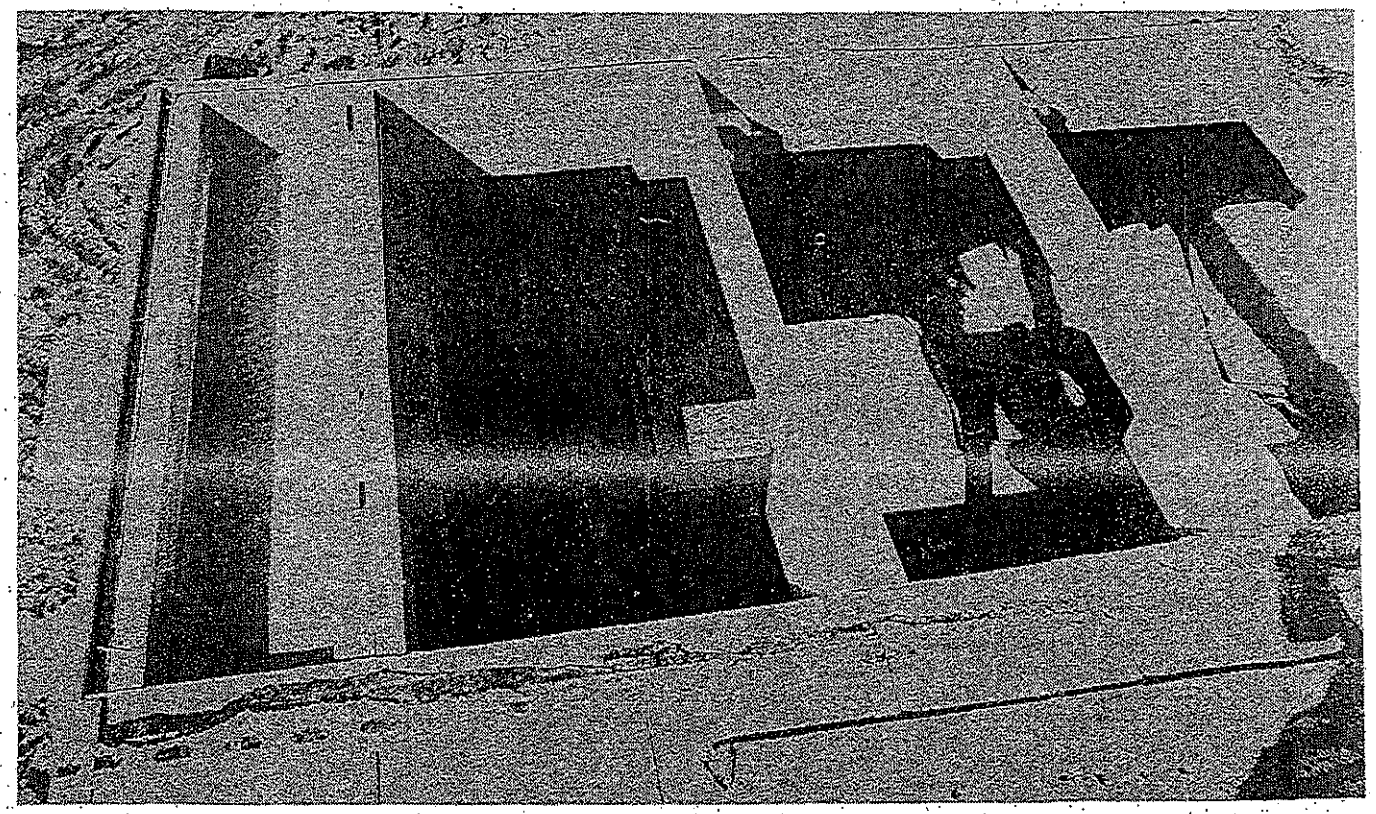

FIGURE 10. - Installed south-end shaker.

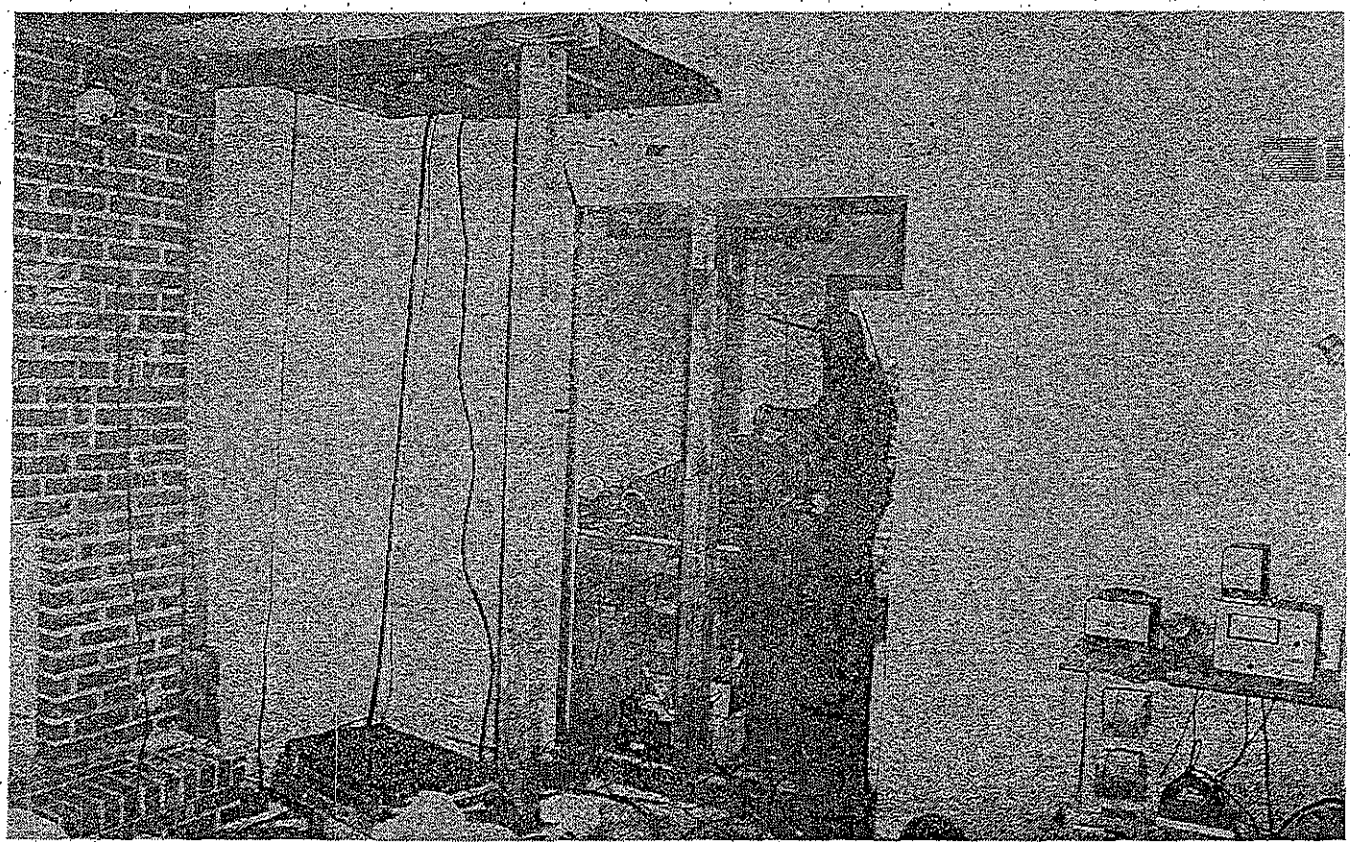

FIGURE 11. - North-end shaker support.

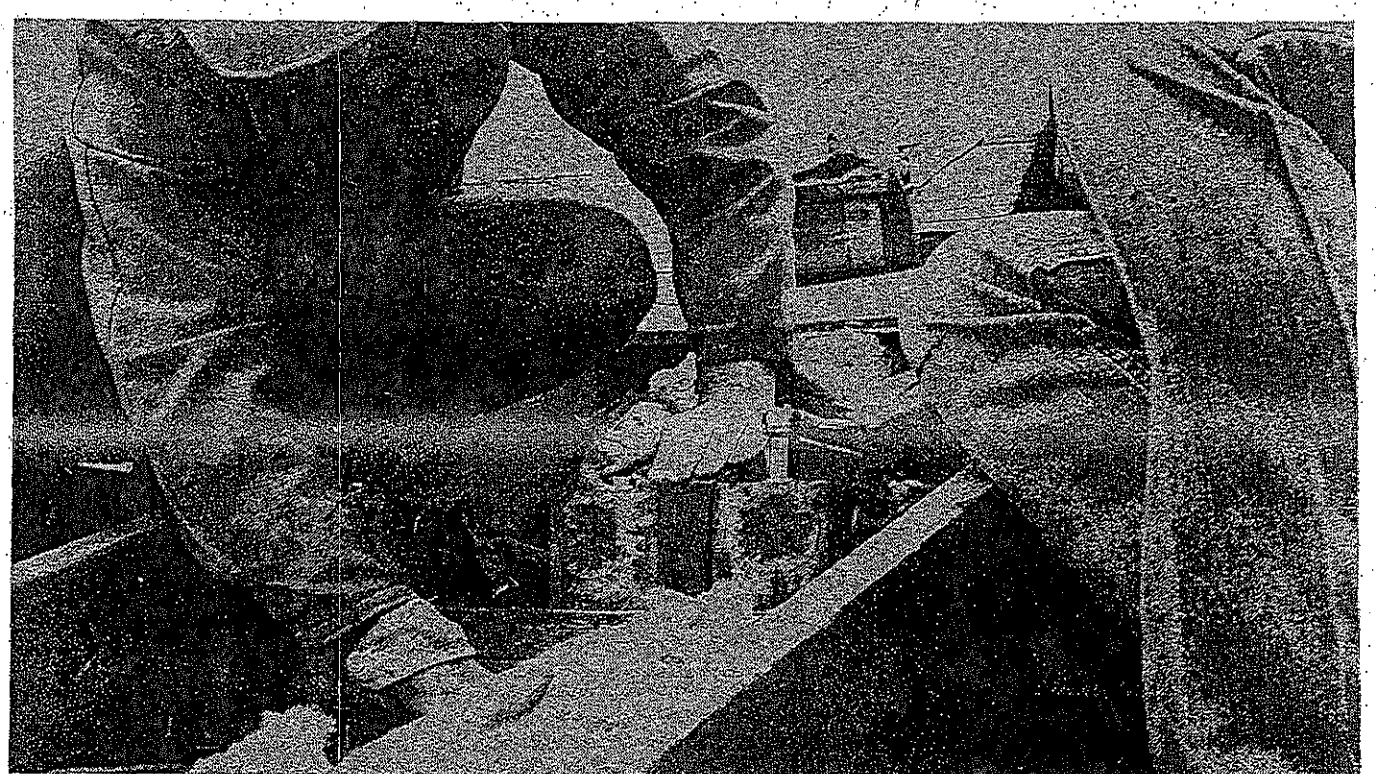

FIGURE 12. - Ceiling joists being bolted to wall studs.

INSTRUMENTATION AND MEASUREMENTS AT TEST HOUSE

A large variety of measurement techniques was needed to quantify strain-producing environmental changes with cyclic periods that ranged from 0.02 s (e.g., blasting) to 1 yr (e.g., seasonal temperature and humidity). Table 4 summarizes the instruments used in the monitoring program. The listed accuracies represent the combined limitations of the instruments and the least division of the chart papers. Locations of all instrumentation are shown in figures 13-16.

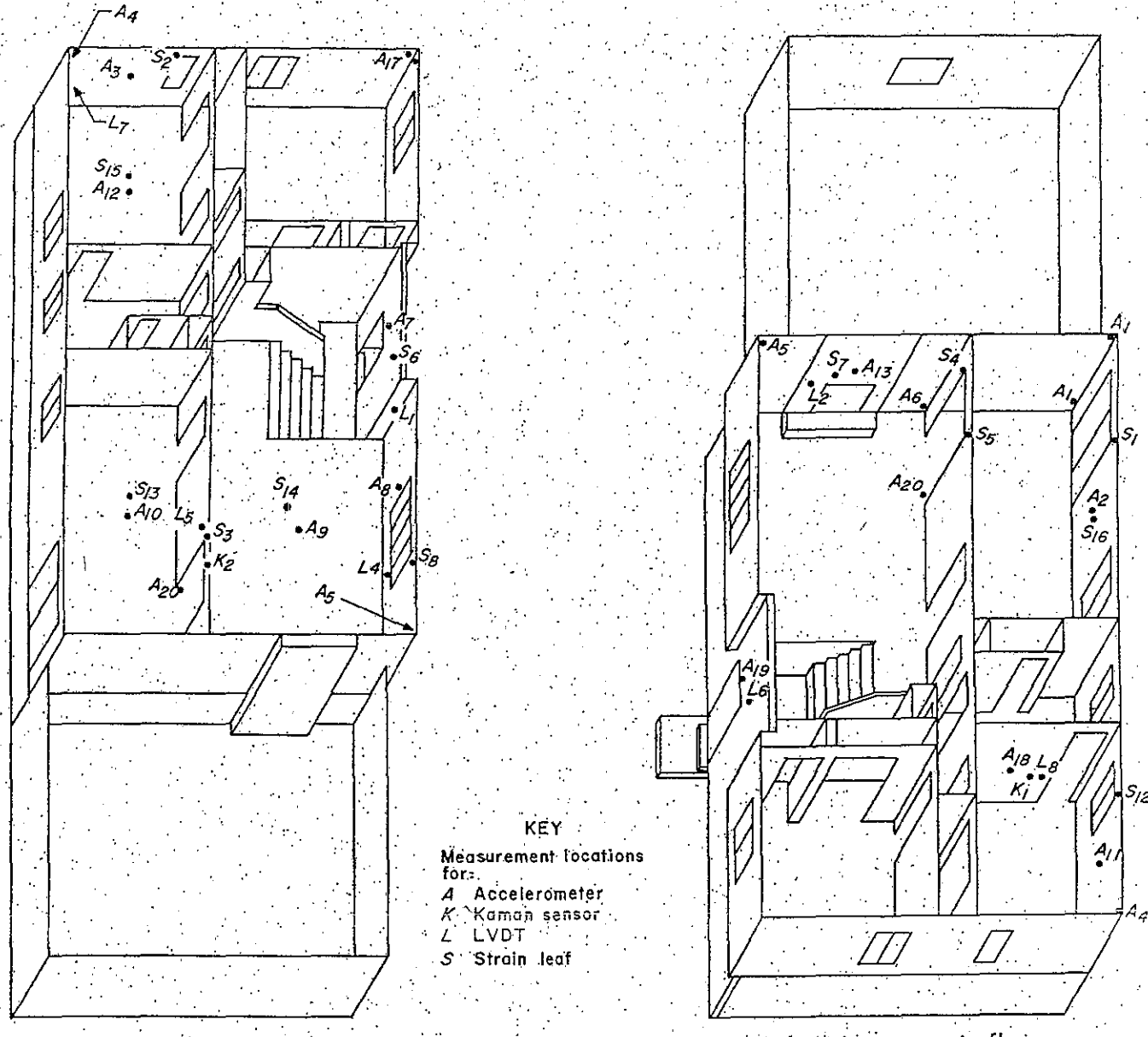

FIGURE 13. - Accelerometer and strain system measurement locations on main floor.

TABLE 4. - Field measurement program for assessing strains and cracking from blasting, household activities, and environmental factors

Measurement	Instrumentation[1]	Accuracy	Number of readings		
			Semimonthly	Every 3 h	Dynamic
Blast vibrations and airblast.	Dallas Instruments, Inc., ST-4; Geo Space Corp., VLF-LP-3D; Vibra-Metrics Inc., MP-120; Validyne Engineering Corp., DP-7.	See text.....	1,060	6	129
Wind speed and direction.	Weather Measurement Corp., Recording Wind System W 224.	2 mi/h, 7.5° F..	1,830	133	NAp
Humidity:					
Inside.....	American Instruments Co., Hygrosensor L15-1810D with Hygrodynamics Inc., Hygrometer Indicator 15-3001; recorded on Gultan Industries, Inc., Rustrak chart recorder 228.	3 pct.....	83	133	NAp
Outside.....	(Data from Dress Regional Airport, Evansville, IN).	Not known.....	96	133	NAp
Temperature:					
Inside.....	Gultan, Rustrak temperature recorder 2133F137 with temperature sensor 1334.	1° F.....	85	133	NAp
Outside.....	Gultan, Rustrak temperature recorder 2144 with temperature sensor 1332.	2° F.....	85	133	NAp
Structure vibration response.	Vibra-Metrics, MB 120 transducers.....	See text.....	NAp	NAp	1,372
	Bruel & Kjaer Instruments, Inc., 4370 accelerometers with 2635 charge amplifier-integrator.				
	Unholtz Dickie Corp., 1000PA accelerometer with 2216 II signal conditioner.				
Settlement.....	E. Lietz Inc., B-2 Philadelphia automatic level rod with vernier.	0.005 ft.....	470	NAp	NAp
Strain:					
Semimonthly..	Interapid, groove comparitor.....	0.0005 in.....	1,359	NAp	NAp
Do.....	Slope Indicator Co., tape extensometer 51855.....	0.003 in.....			
Every 3 h....	Kaman Sciences Corp., KD-2611 recorded on Gultan Rustrak chart recorder 388.	See table 5.....	NAp	133	NAp
Dynamic.....	Kaman, KD-2611 displacement system; Schaevitz Engineering, displacement transducer; Vishay Intertechnology, Inc., Micro Measurement strain gauges; BLH Electronics strain gauges; Strain-leaf displacement system.	...do.....	NAp	NAp	1,975
Household activities.	(Same as for structure vibration response and dynamic strain.)	See text.....	NAp	NAp	360
(Inspections)..	(Maps and photographs).....	NAp.....	48	NAp	258

NAp Not applicable.

[1]Numbers and letter-number combinations identify specific models.

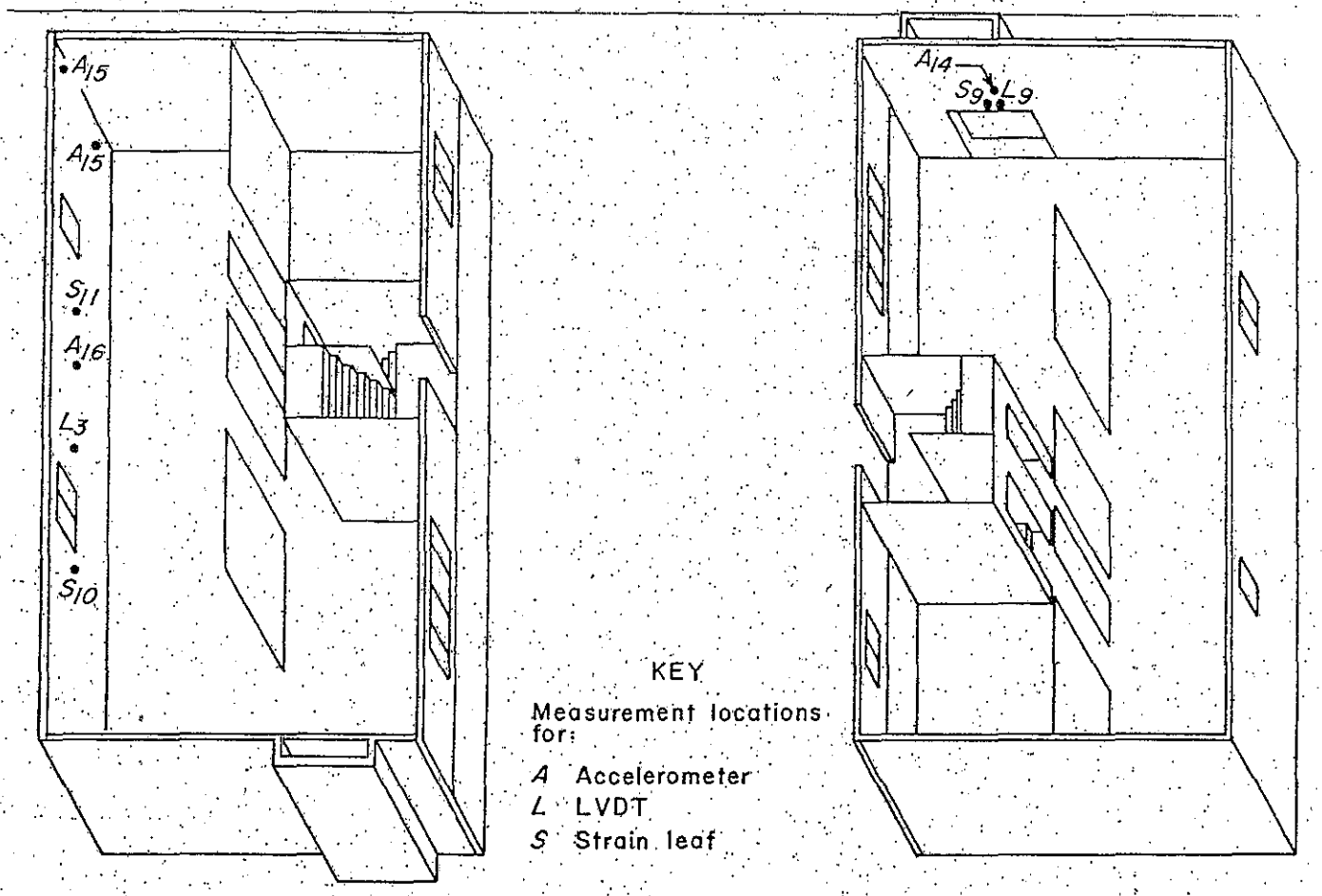

FIGURE 14. - Accelerometer and strain system measurement locations in basement.

Ground Vibration and Airblast

As mentioned earlier, a self-triggered three-component seismograph and airblast monitor recorded every blast from the house-construction phase to field study completion. At times during the study, other instruments were used either next to this reference transducer or at the opposite corner of the house. Up to 12 channels of ground vibration time histories were recorded on magnetic tape for later analysis. This instrumentation is described in detail in two earlier Bureau reports, RI 8506 (29) and RI 8508 (30).

Weather Environment

Weather conditions monitoring was an essential part of this study. Temperature sensors were located both inside and outside the structure. Humidity was measured inside, and wind speed and direction gauges were located on the chimney. All devices were connected to 30-day chart recorders which sampled at 2-s intervals. Additional data were obtained from the Evansville Dress Regional Airport, 5 mi from the test structure.

Household Activities

The dynamic measurement systems also responded to human household activities. Measurements were made of the vibration and strain produced by a variety of normal activities such as walking, jumping, door slamming, and nail pounding.

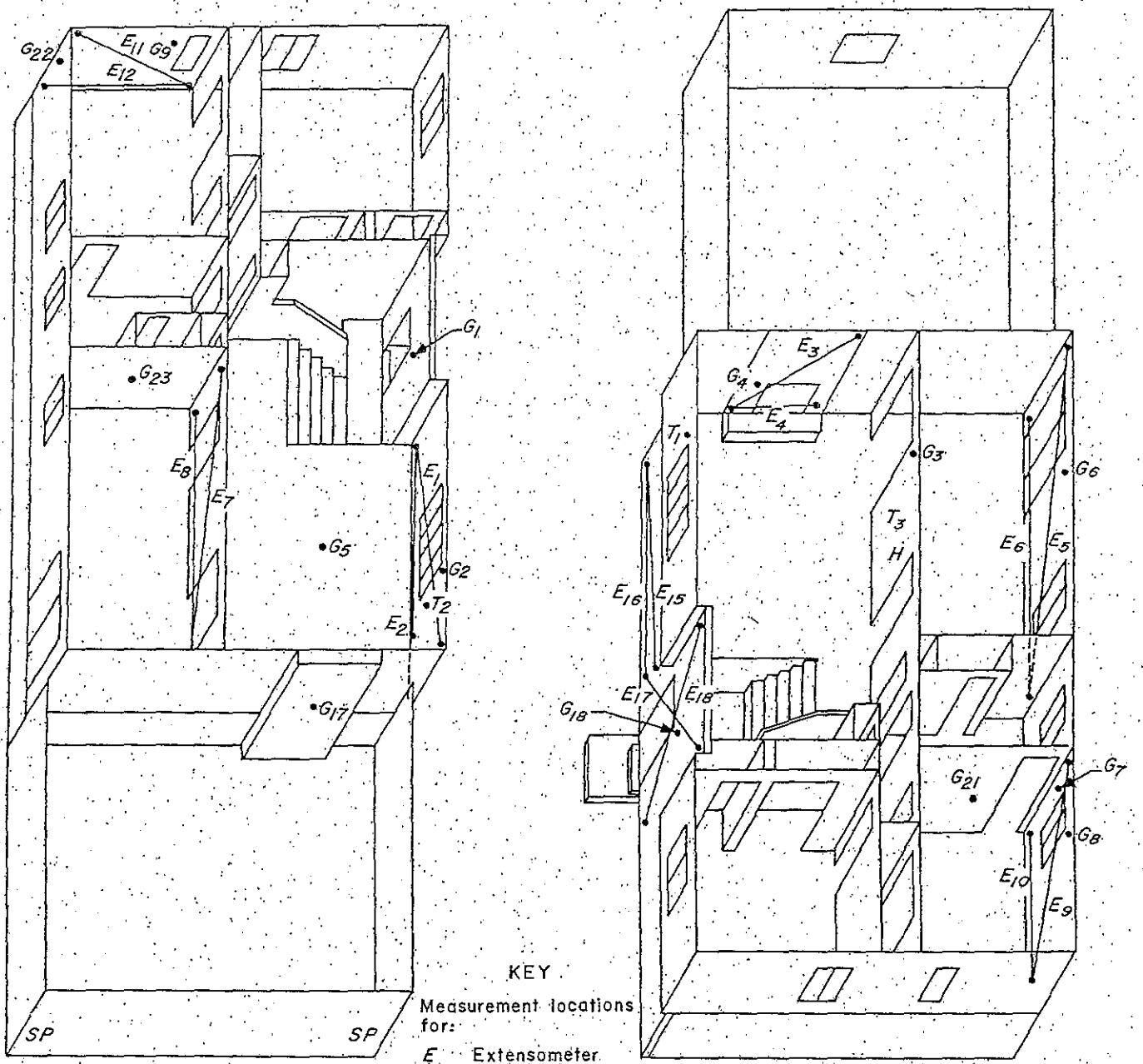

FIGURE 15. - Semimonthly strain, temperature, and humidity measurement locations, and survey points on main floor.

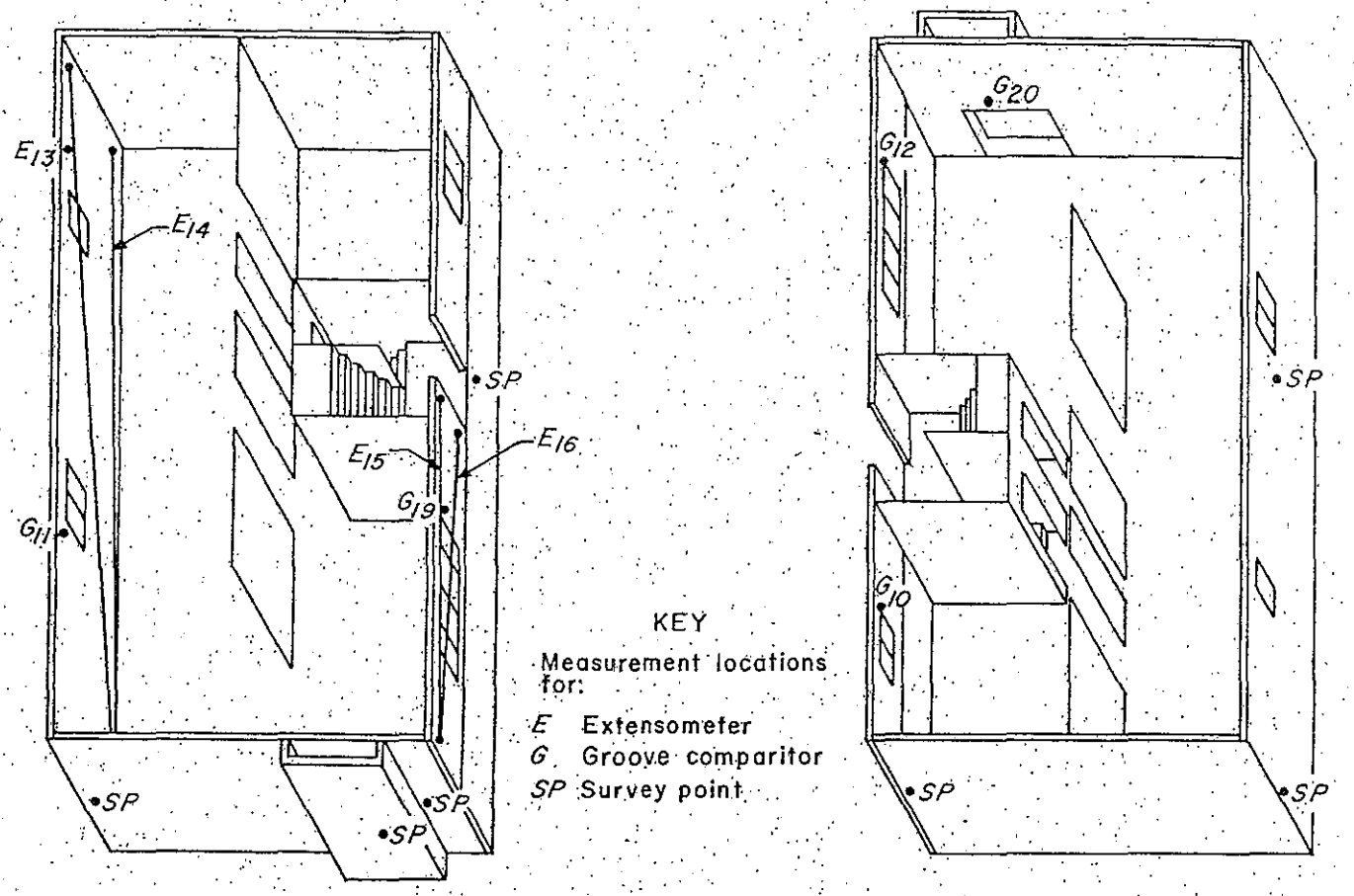

FIGURE 16. - Semimonthly strain, measurement locations, and survey points in basement.

Structure Vibration Response

Structural vibrations produced by blasting and other transient phenomena were monitored using methodology that was similar to, but more complete than, that used in the studies described in RI 8485 (1) and RI 8507 (2). Inside the house, vibration responses were measured at corners (high and low points) and at midwall, midfloor, and midceiling locations. A total of 14 recorder channels was used to record structural vibration. Varying the transducer configuration raised the total number of measuring points to 20. These points are shown in figures 13 and 14 as the accelerometer measurement locations (A_1, A_2, A_3, etc.). At each corner location, up to four measurements were made; these were designated as "high" or "low" (near the ceiling or near the floor) and according to their direction (north, east, etc.). The large number of channels allowed a more complete analysis than was possible in previous studies. Measurements in opposite corners allowed determination of rotational versus translation vibrational modes.

Settlement

Differential settlement of the structure was determined by measuring elevations at the survey points (*SP*) shown in figures 15 and 16. The elevation rod rested on a stainless steel sphere which was welded to a stainless steel stud and grouted into the top course of the block wall. A brass bench mark obtained from the U.S. Geological Survey was installed 50 ft from the house so that each elevation survey would complete a closed loop around the house and thereby identify any differential settlement.

Static Strain and Deformation

Long term changes in static structural strain measurements are affected by gauge length, mounting method, and the long term stability of the equipment. The laboratory tests of gauge length and mounting method described in appendix A indicated a need for a wide range of instrumentation.

The extensometer (fig. 17) and groove comparitor (fig. 18) measured the distance between set reference points ~ 10 to 30 ft apart and ~ 3 in apart, respectively. The reference points for these two devices were permanently mounted stainless steel spheres and dimpled steel blocks. They were installed over critical areas of interest as detailed in figures 15 and 16 (points G_1, G_2, G_3, etc.). Differences in length, between that measured initially and at any later time, were divided by the initial length to obtain the strain values. A 45° rosette was employed at each groove comparitor location on wallboard; and for masonry joints, both the vertical and horizontal axes of the block or brick were instrumented. (Sites G_{13}-G_{16} (masonry locations) are not shown because the reference blocks dislodged after 2 months; however, these sites were promptly replaced by sites G_{17}-G_{20}. G_{21}-G_{23} were additional sites instrumented during installation of the replacement sites.) In all, a total of 49 groove comparitor measurements and 17 extensometer measurements were made each semimonthly data collection period. (Use of site E_{14} was discontinued after 3 months due to loosening of the reference sphere.) Readings were corrected for temperature differences as determined with Invar-bar standards.

Dynamic Strain

Strain measurements were made at 26 locations throughout the test house (points K_1-K_2, L_1-L_9, S_1-S_{13}, and S_{15}-S_{16} in figures 13 and 14; the gauge at site S_{14} failed). All major perimeter walls were monitored with gauges on inside surfaces. Gauges were also mounted over those doorway arches and window openings that were assumed to be areas of highest stress concentrations. Differential motion at the corners was measured by displacement gauges. Strain systems were also mounted across brick and block mortar joints at the fireplace (upstairs and downstairs) and on the outside across the brick veneer mortar joints.

The dynamic strain instrumentation is described in detail in table 5. The Kaman sensor, linear variable-differential transformers (LVDT's), and stain-leaf displacement systems required mounting fixtures. These devices are shown in figures 19-21, respectively. Resistance-wire strain gauges were applied directly to the wall covering materials. Time and care were required to mount the strain gauges. Even with a dummy gauge, constant balancing was necessary to adjust for temperature and electronic drift. Such requirements made field use of the strain gauges tedious and difficult. These problems were reduced by using a system of four strain gauges installed on a metal leaf in a complete bridge arrangement; these gauges were employed in a 45° rosette pattern to allow calculation of principal strains at wallboard locations.

Two LVDT's with custom-made amplifiers were used to record differential movement across block and brick joints and crack openings, especially outside the house. Low-gain amplifiers were required to boost output voltages to desired levels.

Two Kaman systems, which are inherently stable against temperature changes and electronic drift, were used during the last 6 months of the study. They documented displacement measurements on chart recorders (hourly measurements) and recorded vibrations from blasting (dynamic measurements). Earlier efforts to monitor hourly strain failed because of LVDT drift and lack of sensitivity of the groove comparitor. Calibration of the Kaman system for temperature changes consisted of mounting the system on an aluminum bar and comparing theoretical and measured values for length change at various known temperature differences. Over temperature range of interest, 50° to 90° F, errors were less than 10 pct.

TABLE 5. - Dynamic strain measurement systems

(Millimeters except where otherwise specified)

Sensor	Model	Nominal linear range	Sensitivity	Frequency range, Hz	Linearity	Thermal sensitivity, mm/°C	Resolution	Stability	Effective length
Schaevitz LVDT[1]	050 GCD	±1.25	[2]~8 V/mm	[3]0- 100	[4]<±0.00625	0.0063	0.000635	0.00318	25
	250 GCD	±6	~1.6 V/mm	0- 100	<±.015	.0013	.000635	.0159	25
	050 HCD	±1.24	[2]~8 V/mm	0- 500	[4]<±.00625	.0063	NA	.00318	25
Kaman KD-2611: Eddy current	0.25S	0.25	~10 V/mm	0-50,000	<±.00125	<±.004	.0001	<±.003	25-90
Displacement system	1U	1	~1 V/mm	0-50,000	<±.005	<±.004	.0001	<±.001	25-90
BLH: Strain gauge	A-9-3UF-120	40,000 μin/in	~0.005 V/με	NA	REF	REF	NA	REF	~124
Semiconductor strain gauge	SPBI-35-500	[5]75 μin/in	~0.02 V/με	NA	REF	REF	NA	REF	~9
Micromeasurement strain leaf system	Ea-13-125Bz -350	±0.10	[6]~0.005 V/mm	>0- 100	NA	NA	<.0002	NA	15-90

NA Not available.
REF Reference company specifications.
V/με Volt per microstrain.
[1]Linear variable differential transformer.
[2]With Bureau amplifier output up to 80 V/mm.
[3]Upper frequency limit specified at 10 Hz; shake table calibrated to 100 Hz.
[4]Individual test = ±0.002 mm.
[5]Limited to amplifier output.
[6]With Bureau amplifier output from 25 to 250 V/mm.

FIGURE 17. - Extensometer.

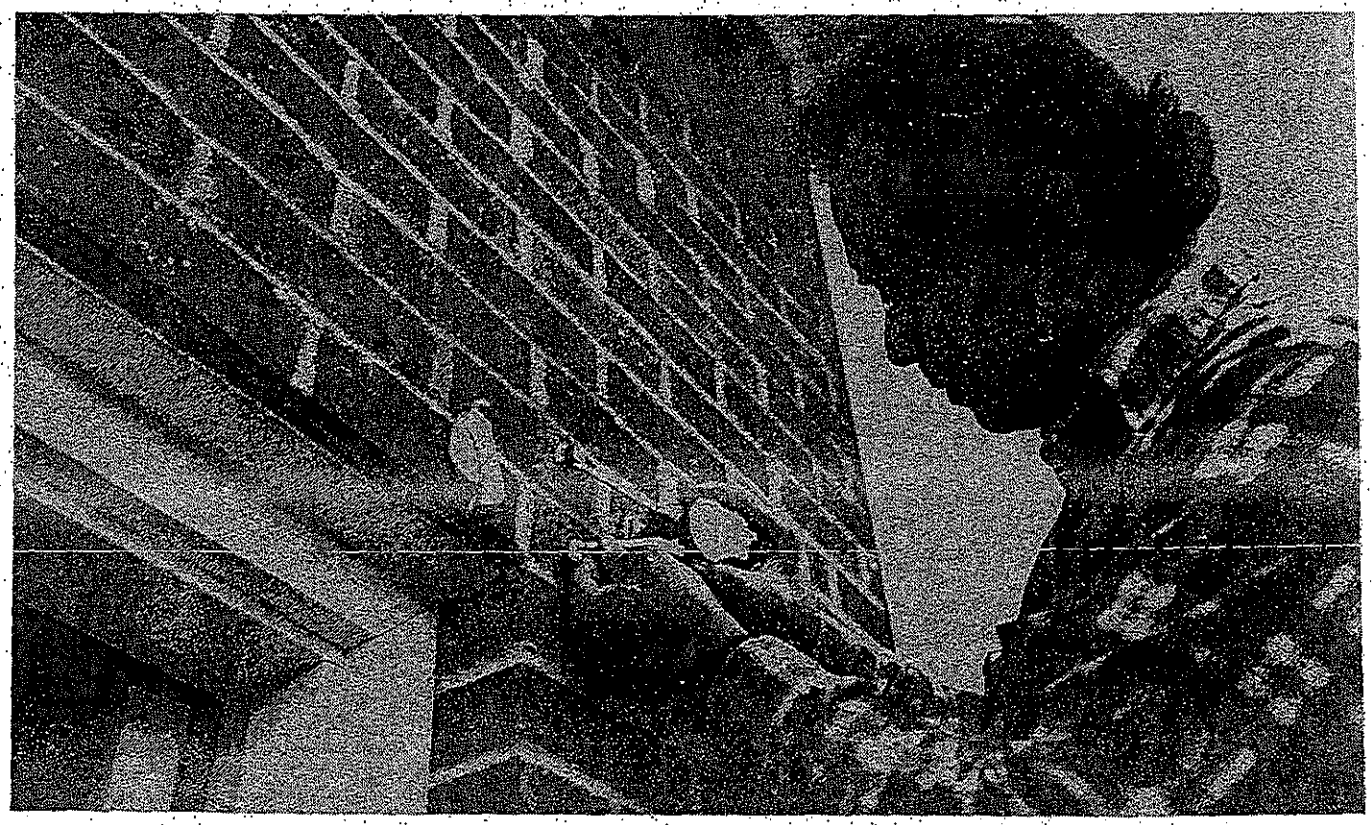

FIGURE 18. - Groove comparitor.

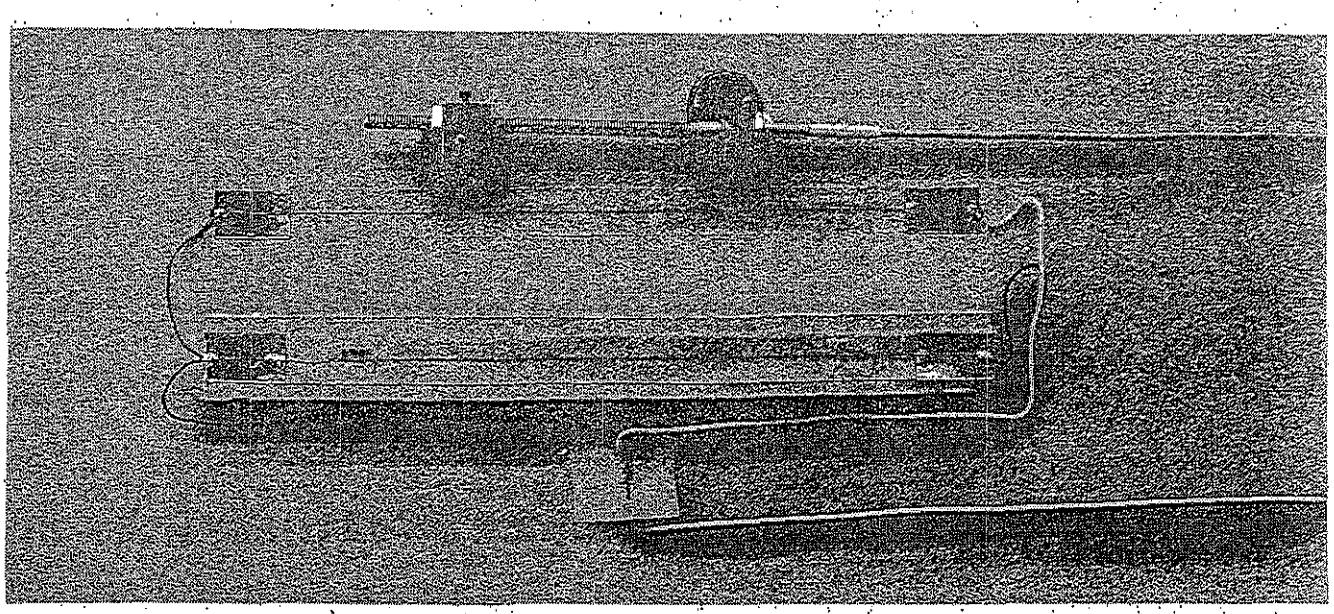

FIGURE 19. - Kaman displacement system (top) and 124-mm strain gauge.

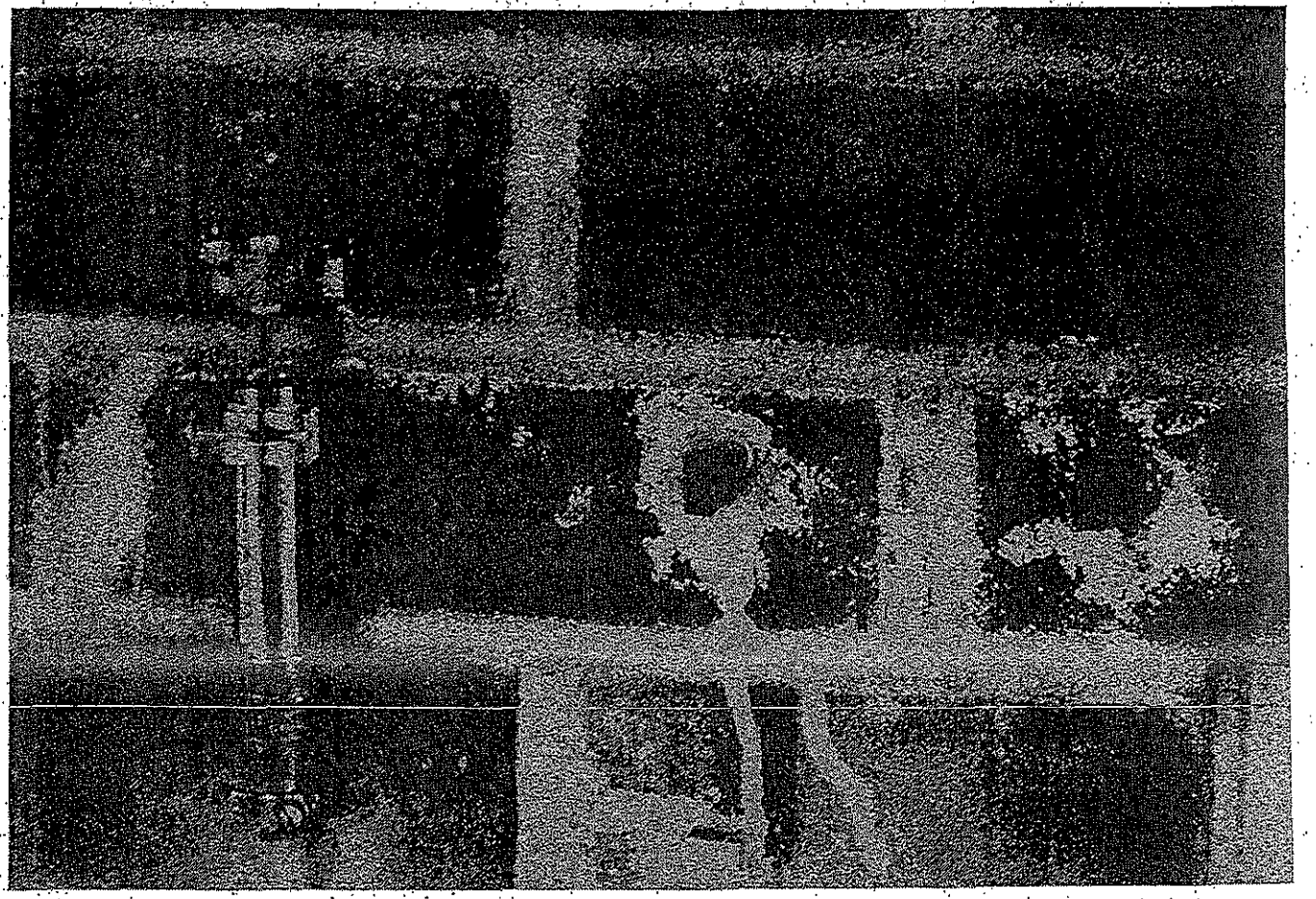

FIGURE 20. - LVDT.

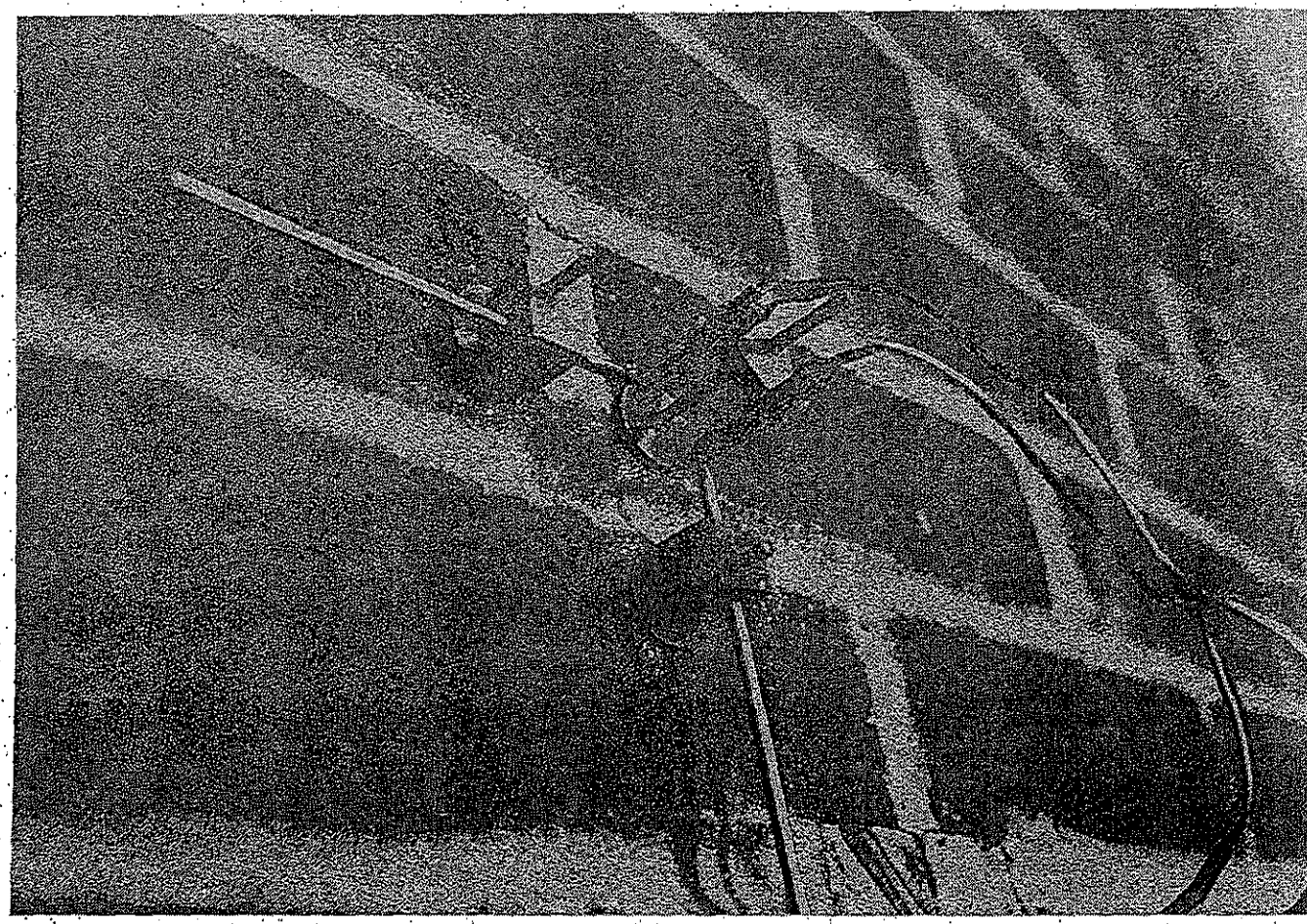

FIGURE 21. - Strain-leaf measurement system.

Of the 50 FM channels available for recording dynamic data, 27 were usually used for recording strain time histories (16 strain leaf, 9 LVDT, and 2 Kaman). A variety of gauges installed in the master bedroom is shown in figure 22. Before and after the study, a frequency response calibration, from 2 to 100 Hz, was performed on all systems using the Bureau's 300-lbf shaker system, as described in RI 8506 (29).

Visual Inspection

Crack inspections were conducted throughout the study. During each inspection, crack extension endpoints were marked and the map of cracks at the termination of construction was updated for all crack extensions, nail pops, and new cracks. Two inspectors documented any extensions, new cracks, or nail pops visible to the naked eye, using a trouble light to highlight the visible features. In addition, very detailed inspections were conducted twice each month by VME personnel. They made pre- and post-blast inspections whenever dynamic readings were taken. The time between shots on the same day was sometimes limited, so the inspectors documented material cracking according to an established plan. When vibrations greater than 1.0 in/s were expected, Bureau personnel were also present to document cracking and assist in monitoring.

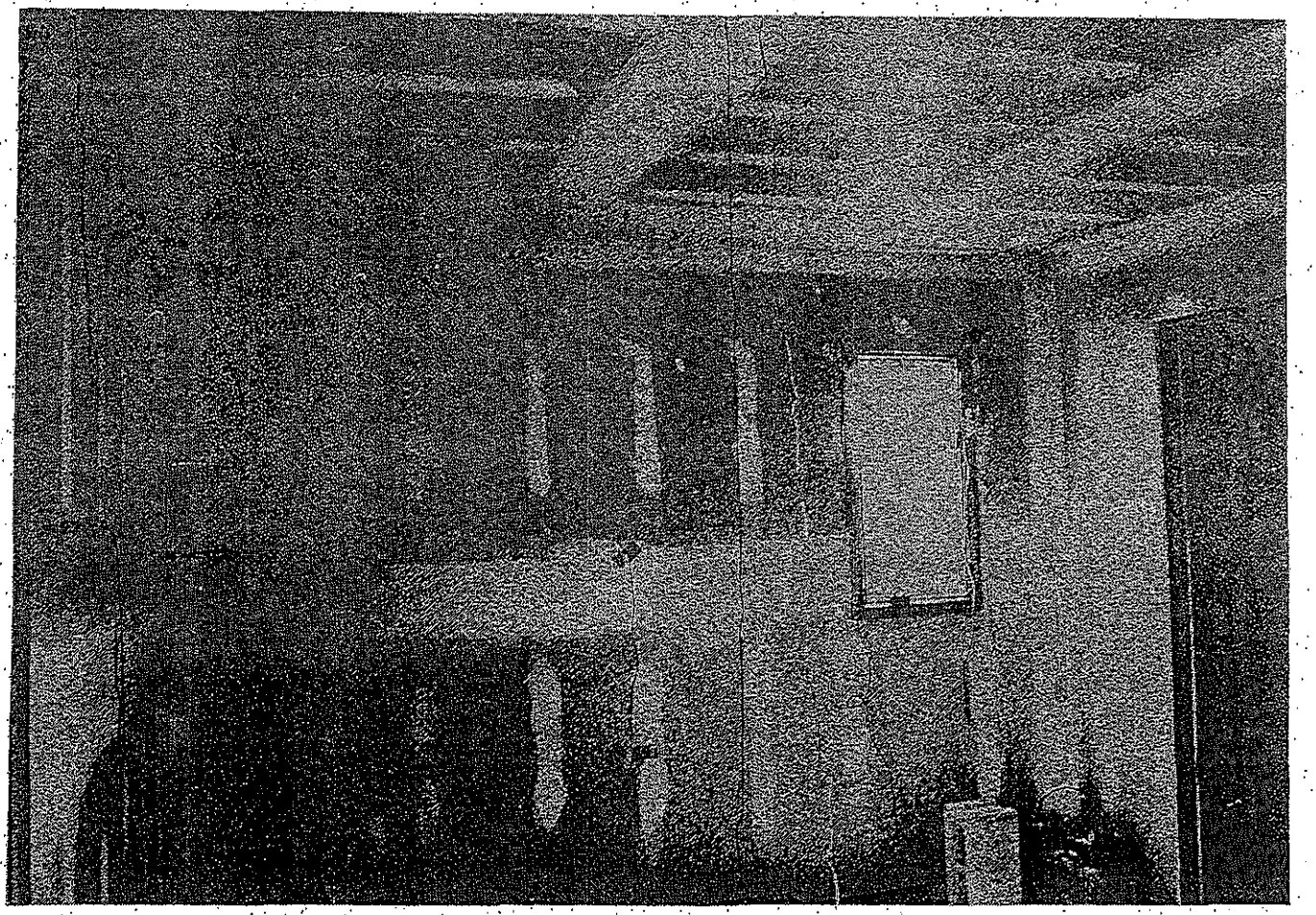

FIGURE 22. - Measurement systems in master bedroom.

RESULTS

The results of this study are discussed with the following objectives:

1. To compare strain levels produced by blasting with those induced by natural events.

2. To describe how these natural and manmade events combine to cause cracking in a house.

3. To document the effect of blasting on the crack rate for the test house.

STRUCTURE RESPONSE TO NATURAL PHENOMENA

Insight into the potential of blasting to induce cracking was gained from comparison of strains produced by vibrations and natural events with the strain level at which wallboard failure occurs. The strain level required for wallboard failure was determined from laboratory testing. Previous research and the latest Bureau tests (appendix A) show first cracking of composite wallboard to occur around 1,000 to 1,200 μin/in, regardless of the mode of failure (bending or tension) and rate of loading. Table 6 lists the strains induced in the test house walls in response to various natural (i.e., nonblast) events; for each event, it also lists the corresponding blast vibration level. A detailed discussion of the structure responses to the events listed in table 6 follows.

TABLE 6. - Comparison of strain levels induced by daily environmental changes, household activities, and blasting

Loading phenomena	Site[1]	Induced strain, μin/in	Corresponding blast vibration level,[2] in/s
Daily environmental changes.	K_1	149	1.2
	K_2	385	3.0
Household activities:			
Walking.....	S_2	9.1	.03
Heel drop.....	S_2	20.0	.03
Jumping.....	S_2	37.3	.28
Door slam.....	S_1	48.8	.50
Pounding a nail....	S_{12}	88.7	.88

[1]From figure 13.

[2]Based on envelope line of strain versus ground vibration plot.

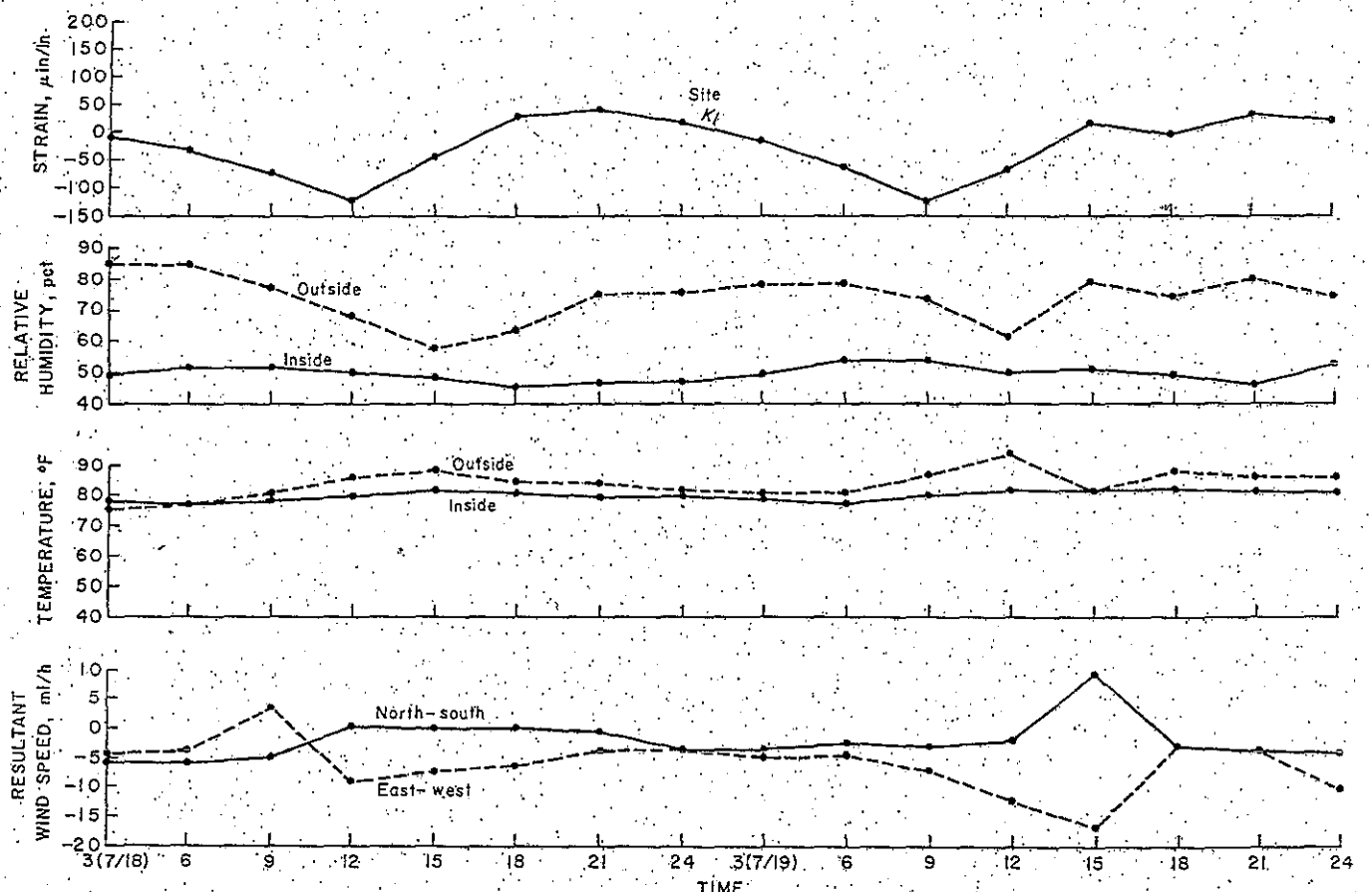

FIGURE 23. - Strain and environmental factors versus time, site K_1.

Response to Daily Environmental Changes

The Kaman displacement system, which has high stability with respect to temperature changes and electronic drift, was used to monitor prestrain resulting from cyclic changes in temperature, humidity, and wind. Two monitoring locations were chosen across taped joints (K_1 and K_2 in figure 13). Site K_2 was in an area of possible high stress concentrations.

Readings were taken in 3-h increments. Figures 23 and 24 display the data for a 2-day period. Because the strain was produced by at least four environmental factors, multiple linear regression analysis was used to quantify the factors.

$$\text{Strain} = C_o + C_1X_1 + C_2X_2 + C_3X_3 + C_4X_4,$$

where C_o and C_1, C_2, C_3, and C_4 are the intercept and coefficients and X_1, X_2, X_3, and X_4 are the humidity, temperature, wind, and ground vibration data, respectively. Assuming normal distribution, a t-test was applied at the 10-pct significance level to eliminate factors. (That is, when t values were greater than 1.71 for site K_1 and 1.65 for site K_2, the null hypothesis that the coefficient of the factor = 0 was rejected.) The t-test statistically evaluated wind, temperature, humidity, and vibration for their degree-of-fit with the resulting strain. If one of these factors did not fit 90 pct of the time, it was dropped from the equation. Several combinations were investigated, including humidity as a time-delayed effect. When variables could be eliminated, coefficients were recalculated. Coefficients and statistics for the three equations with the best correlations are

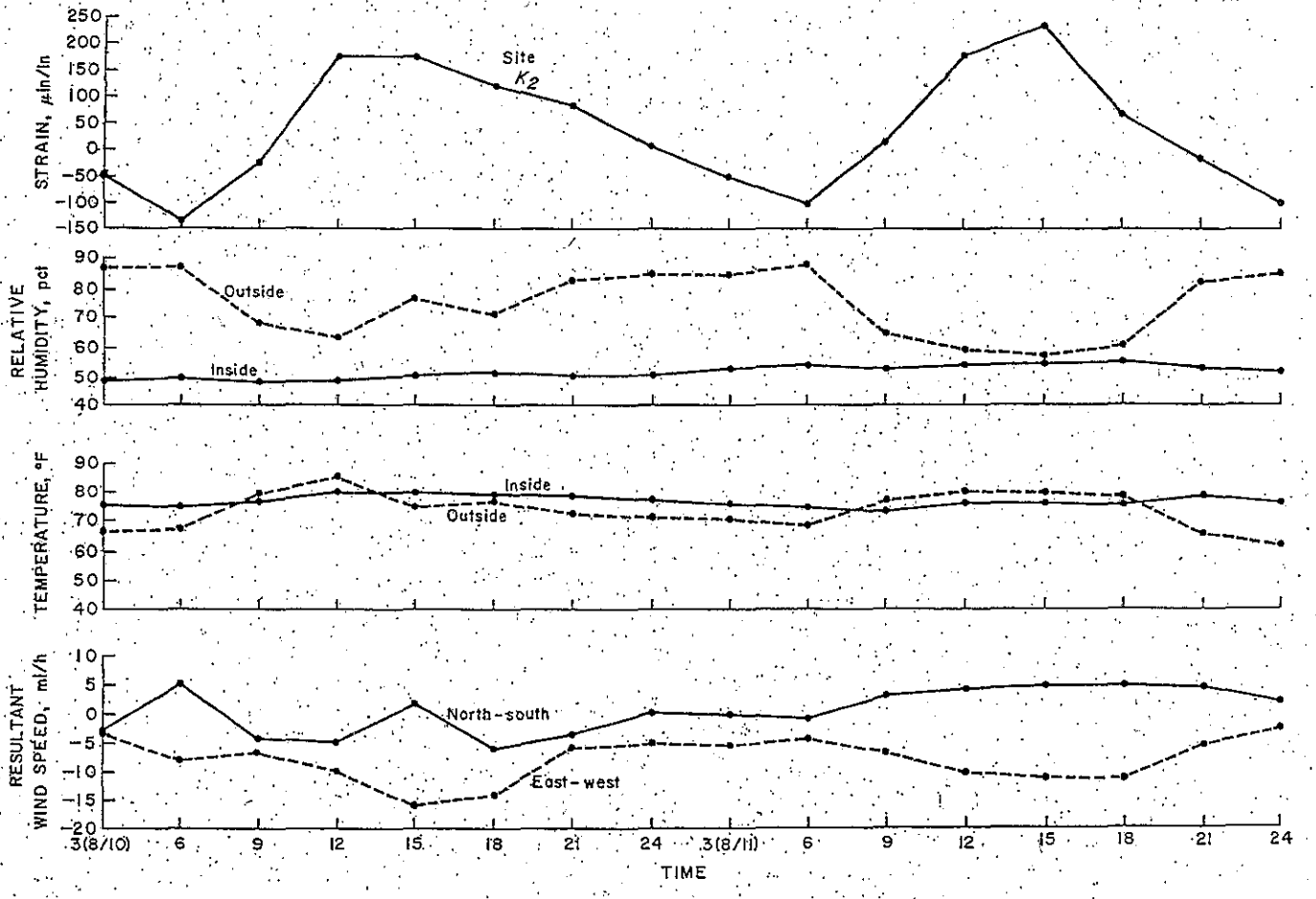

FIGURE 24.- Strain and environmental factors versus time, site K_2.

given in table 7. For example, the microstrain ($\mu\varepsilon$) at site K_2 from equation 2 is equal to

$$-4010 + 6.28\,(RH_I) + 9.24\,(RH_o) + 21.0\,(T_I) + 18.9\,(T_o) + 8.24\,(W_{N-S}) - 2.28\,(W_{E-W}) \pm 86.0\,(Z),$$

with $R = 0.7524$,

where RH_I = relative humidity inside, pct,

RH_o = relative humidity outside, pct,

T_I = temperature inside, °F,

T_o = temperature outside, °F,

W_{N-S} = wind speed from north to south, mi/h,

W_{E-W} = wind speed from east to west, mi/h,

Z = number of standard deviations,

and R = correlation coefficient.

The ground vibration factor dropped out of the equations because the data were taken during periods of little blast activity. The best fit for site K_2, equation 3, with $R = 0.7653$, utilized a lag of the inside humidity; i.e., the 3, 6, and 9 o'clock readings became the 6, 9, and 12 o'clock readings, etc. Equation 2 provided a comparison of the strains at sites K_1 and K_2 based on the unlagged data. Although some environmental variables dropped out for site K_1 (equation 1), they were all present at K_2 (equations 2 and 3). The correlations were apparently valid because the wind perpendicular to the wall produced the major strain response (shear) at the monitored interior walls.

Strain resulting from each environmental factor can be predicted by multiplying the range of the factor by the factor's coefficient. For example, the 13-pct change in relative humidity could produce a maximum strain of 202 μin/in $\left(\frac{15.5\ \mu\varepsilon}{RH,\ pct} \times 13\ pct\right)$. Ranges of each factor and corresponding maximum strains are presented in table 8.

TABLE 7. - Coefficients and statistics[1] for strain induced by relative humidity, temperature, and wind

Factor	Equation 1		Equation 2		Equation 3	
	C + S	t-value	C + S	t-value	C + S	t-value
Relative humidity:						
Inside.....	15.5 ± 1.61	9.61	6.28 ± 2.65	2.37	[2]9.40 ± 2.82	3.33
Outside.....	NAp	NAp	9.24 ± 1.12	8.26	9.31 ± 1.09	8.55
Temperature:						
Inside.....	NAp	NAp	21.0 ± 4.93	4.25	18.3 ± 4.81	3.80
Outside.....	6.40 ± 1.16	5.54	18.8 ± 2.15	8.76	19.7 ± 2.08	9.48
Wind:						
North-south.....	NAp	NAp	8.24 ± 2.60	3.17	6.24 ± 2.68	2.33
East-west.....	1.77 ± 0.867	2.04	-2.28 ± 1.20	-1.90	-3.02 ± 1.20	-2.50

C Coefficient.
S Standard deviation.
NAp Not applicable; i.e., factor not statistically significant.
[1]Equation statistics:

	Equation 1	Equation 2	Equation 3
Intercept ± S..	-1,240 ± 25.7	-4,010 ± 86.0	-4,030 ± 83.8
Correlation coefficient...	0.7822	0.7524	0.7653

[2]Inside relative humidity for equation 3 was best fit by lagging data 1 period.

TABLE 8. - Predicted increase in strains at sites K_1 and K_2 (fig. 13) from maximum observed changes in relative humidity, temperature, and wind

Factor and equation from table 7	Range of factor	Strain, μin/in
Inside relative humidity:		
1	44-57 pct	202
2	40-59 pct	119
3	40-59 pct	179
Outside relative humidity:		
2	53-88 pct	323
3	53-88 pct	326
Inside temperature:		
2	70°-82° F	252
3	70°-82° F	220
Outside temperature:		
1	74°-92° F	115
2	59°-86° F	508
3	59°-86° F	532
North-south wind:		
2	N 14.1, S 8.81 mi/h	189
3	N 14.1, S 8.81 mi/h	143
East-west wind:		
1	E 5.31, W 18.79 mi/h	42.7
2	E 14.77, W 16.02 mi/h	-70.2
3	E 14.77, W 16.02 mi/h	-93.0

Strains from daily environmental changes could cause core failure or possible paper cracking. The maximum strains observed at K_1 and K_2 were +149 and +385 μin/in, respectively. The total maximum strains calculated from the correlation equations 1-3 (as described in table 7), assuming the worst case for each of the factors, were +242 to -118, +665 to -796, and +675 to -817 μin/in, respectively. Assuming linear response, strain values at an adjacent location would be similar to strains across the monitored taped joints. Since wallboard was observed in the laboratory to crack at 1,076 to 1,420 μin/in, it can be concluded that a confluence of environmental effects only slightly greater than those indicated by the last two ranges given above (from equations 2 and 3) would be sufficient to crack wallboard. In fact, one of the authors observed the occurrence of a wallboard crack in his own home directly over a doorway on a cold winter evening (20° F outside temperature) during a period of minimum humidity and temperature--both conditions that lead to maximum stress.

Minimum blast vibrations of 1.2 and 3.0 in/s would be needed to produce the 149- and 385-μin/in microstrains observed at sites K_1 and K_2, respectively. For example, the K_2 equivalency can be found from the envelope line for the strain versus maximum ground vibration at K_2 as plotted in figure 25.

Response to Monthly Environmental Changes

Monthly environmental data were collected from groove comparitor and extensometer readings but were not used in the final analysis because in some cases calculated strains should have produced cracking, and in other cases not enough data were collected to permit a valid statistical analysis. The data were ambiguous. Extensometer readings at locations E_1 and E_2 (fig. 15) gave conflicting results. For example, for strains

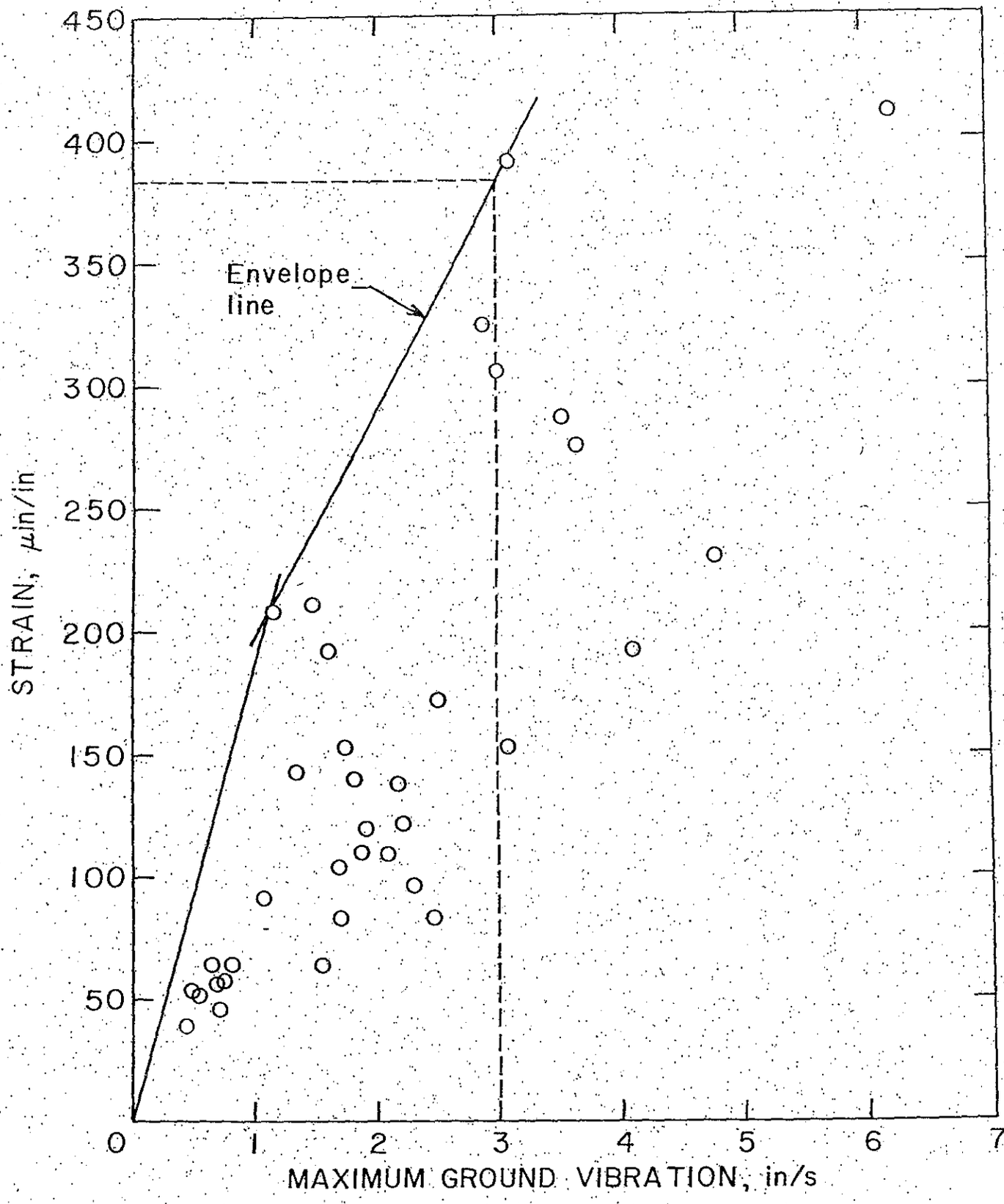

FIGURE 25. - Strain versus maximum ground vibration level, site K_2.

read over virtually the same structural area, multiple linear regression analysis eliminated the settlement factor for location E_2 but not for E_1. This should not occur for sites on the same wall.

The accuracy of the readings depended largely on operator efficiency, attachment apparatus, and mounting techniques. The groove comparitor readings were highly suspect because of limited gauge accuracy (±100 μin/in) and methodology. Questions arose as to whether comparitor tip alignment was done in the same manner from one period to another and the possibility of foreign matter settling on the blocks where the measuring tips rested. The extensometer required 40 lb of applied tension on the measurement tape, and this pull may have affected strain readings, depending on how well the attachment points were anchored into the wall. The comparitor and extensometer systems were designed to display displacements caused by differential settlement. The results of the level-loop surveying showed that differential settlements observed across the walls were negligible (~ 0.01 in). Because of these uncertainties, long term effects were examined with respect to crack rate changes, which are described in a later section ("Long Term Cracking Observations").

Response to Household Activities

Several human activities such as jumping, door slamming, walking, and nail pounding were monitored at the test house. The results showed that these activities induced strains similar to those induced by ground motions from blasting. Table 9 lists the equivalent ground vibration levels based on comparative strain or structure-motion response. These ground motion equivalencies are based on a worst-case analyses (using an envelope line as shown in figure 26) and on a least-squares regression-line analyses. For example, the strain recorded at location S_1 (fig. 13) by slamming the sliding door was 48.8 μin/in. The equivalent ground vibration levels were read from the plot presented in figure 26, which shows strain versus peak ground vibration at site S_1. The envelope- and regression-line equivalent blast vibration levels are 0.50 and 1.40 in/s, respectively, as indicated by the broken lines in figure 26. The 0.50-in/s value is a worst-case prediction based on strain-producing ground vibration being the independent variable. Blast vibration levels equivalent to human activities are up to 0.88, 0.59, and 0.92 in/s based on envelope analysis (worst case) of strain, structure motion, and midwall response, respectively; and similarly, up to 1.44, 0.90, and 2.16 in/s based on regression-line analysis.

STRUCTURE RESPONSE TO BLAST VIBRATIONS

The strain and structure motion induced in a house by blast vibrations are dependent on the transfer of ground vibration energy through the foundation and the house's wooden framework (superstructure) to the attached wall covering. Airblast induces additional strain and structure motion as it shakes the superstructure. Typical structural strain and velocity time histories measured at corner, midwall, and ground-level locations are shown in figures 27 and 28. High-corner east-wall velocity waveforms A_4 and A_1 are out of phase, indicating that shot 123 subjected the superstructure to torsional motion. Both translational and torsional response were measured, regardless of shot location. Figure 27 illustrates the similarity of waveforms that resulted from the ground motion and those that resulted from the induced structure motion.

TABLE 9. - Human activities and equivalent ground vibration levels

Activity	Location[1]	Induced strain (μin/in) or structure motion (in/s)	Ground vibration equivalency, in/s	
			Envelope[2]	Regression line[3]
Walking.....	A_4, low corner, south wall.	0.16 in/s.....	0.07	0.29
	A_4, low corner, east wall.	0.039 in/s.....	.005	.07
	S_2.....	9.1 μin/in.....	.03	.09
Heel drop.....	A_4, low corner, south wall.	0.14 in/s.....	.06	.24
	A_2, Midwall.....	0.65 in/s.....	.06	.17
	S_2.....	20 μin/in.....	.03	.20
Low jump.....	A_4, low corner, south wall.	0.12 in/s.....	.05	.18
	A_2, midwall.....	1.8 in/s.....	.26	.92
High jump.....	A_4, low corner, south wall.	0.31 in/s.....	.29	.74
	A_2, midwall.....	1.2 in/s.....	.15	.52
	S_2.....	42 μin/in.....	.28	.62
Entrance door slam.	A_4, low corner, east wall.	0.18 in/s.....	.09	.22
	A_3, midwall.....	1.3 in/s.....	.13	.52
	S_8.....	21 μin/in.....	.27	.60
Sliding glass door slam.	A_1, high corner, east wall.	0.87 in/s.....	.51	.90
	S_1.....	48.8 μin/in...	.50	1.40
Sinking nails for pictures.	A_4, low corner, east wall.	0.51 in/s.....	.38	.80
	A_5, low corner, west wall.	0.67 in/s.....	.59	.89
	A_2, midwall.....	3.9 in/s.....	.92	2.16
	S_1.....	21 μin/in.....	.18	.41
	S_8.....	32 μin/in.....	.38	.87
	S_{12}.....	88.7 μin/in...	.88	1.44

[1]From figure 13.
[2]Based on envelope of strain or structure motion versus ground vibration data.
[3]Based on regression line through strain or structure motion versus ground vibration data.

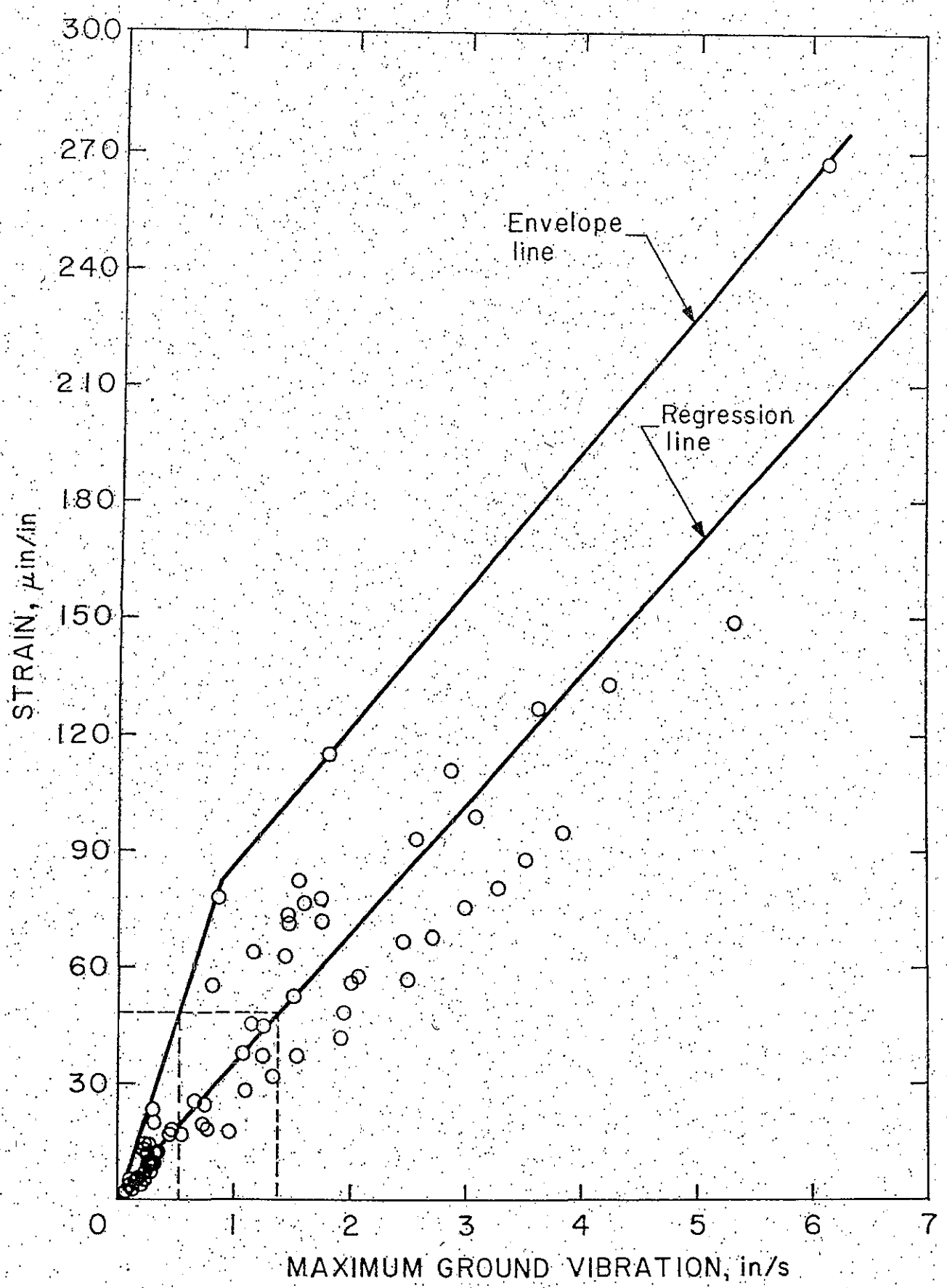

FIGURE 26. - Strain versus maximum ground vibration level, site S_1.

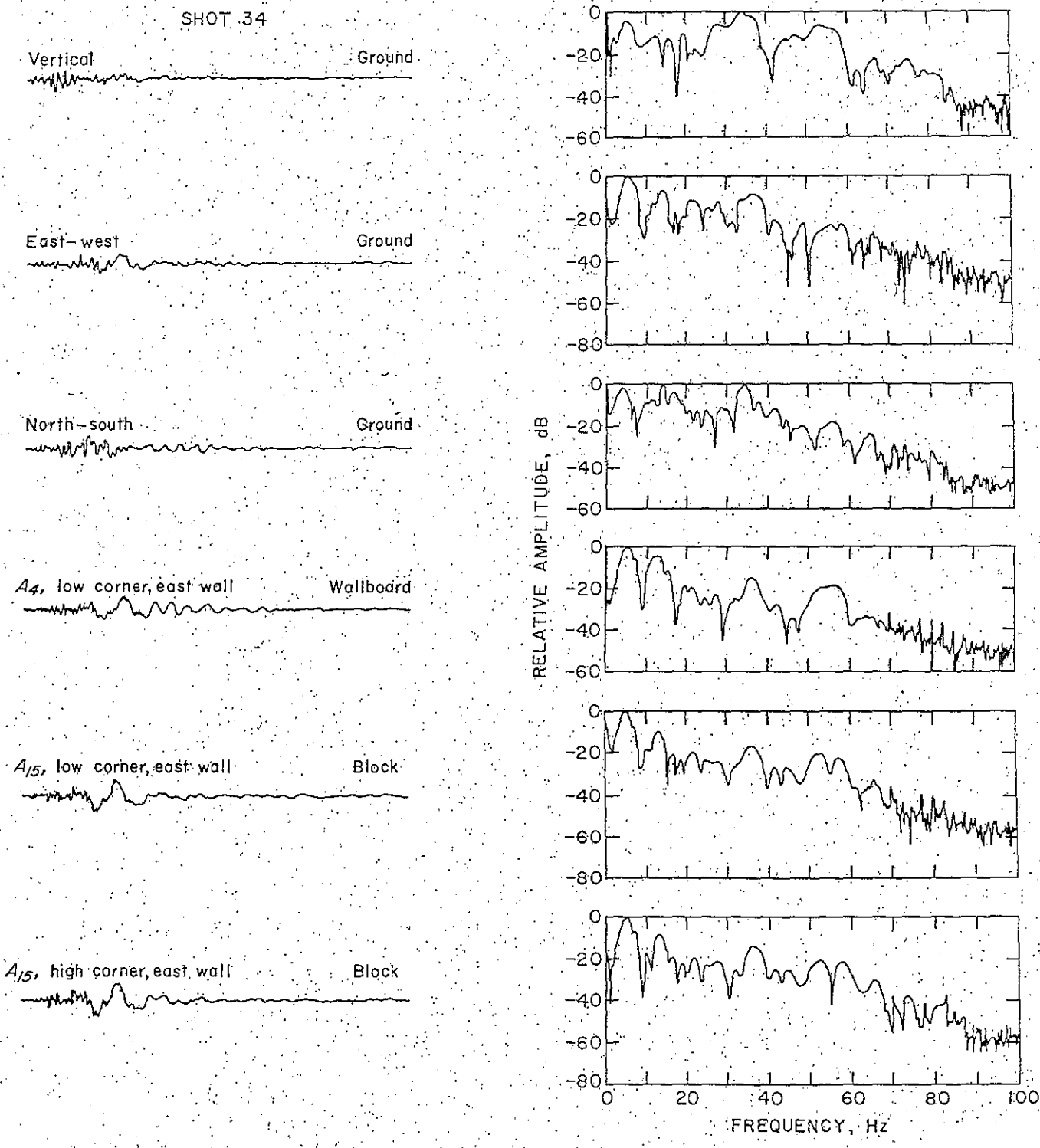

FIGURE 27. - Typical ground vibration and structure response waveforms for shot 34 with corresponding spectra. (Designations such as A_4 correspond to locations shown in figures 13 and 14.)

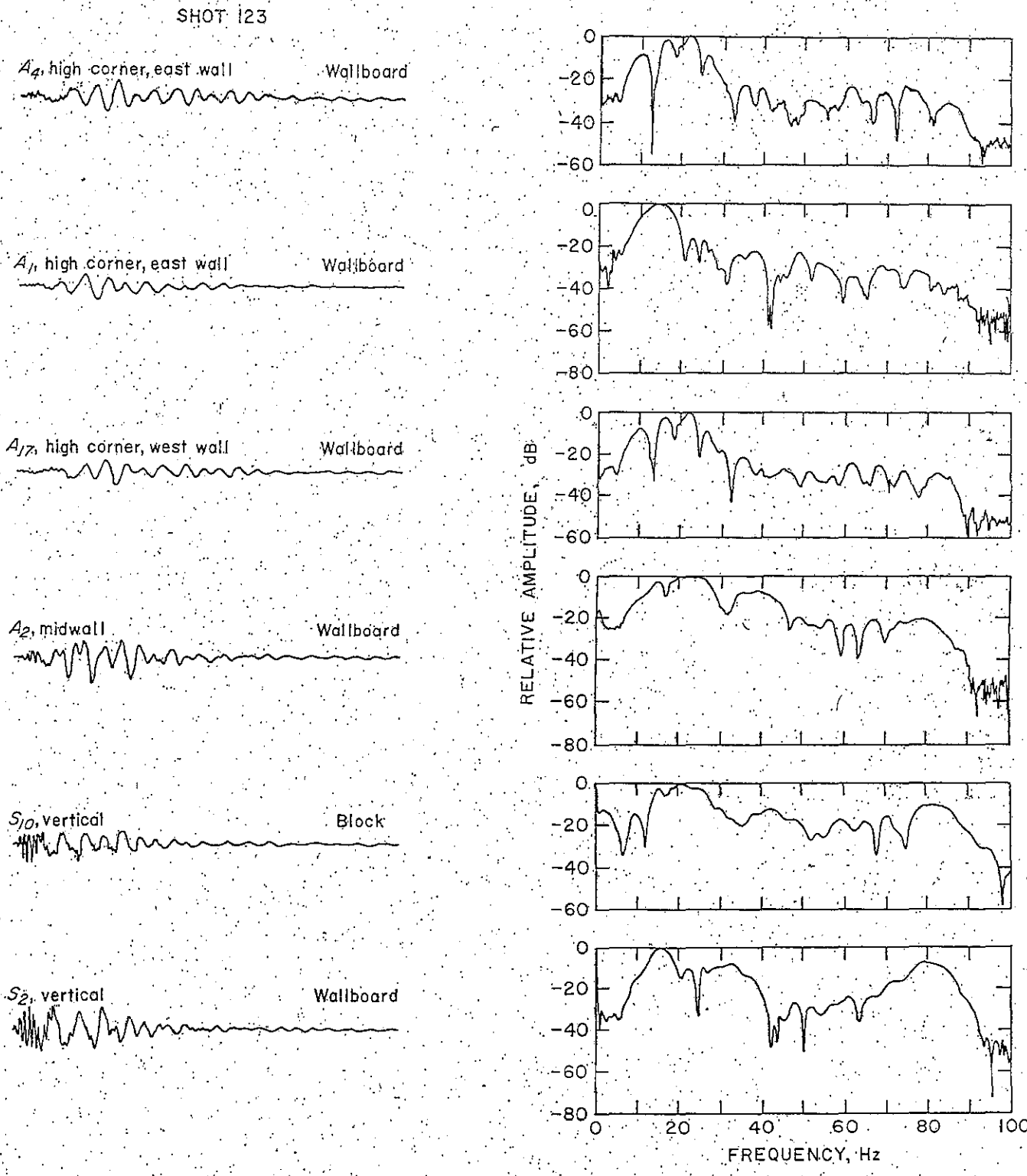

FIGURE 28. - Typical ground vibration and structure response waveforms for shot 123 with corresponding spectra. (Designations such as A_4 correspond to locations shown in figures 13 and 14.)

Low- and high-corner responses are plotted against maximum ground vibration (ground peak particle velocity) in figure 29. A large difference exists in the slopes of the envelopes of the high- and low-corner responses and in the scatter of data. The slope of the envelope of structure motion versus maximum ground vibration is a good approximation of the maximum amplification factor. Structure response depends on the frequency of the excitation. The large scatter of data in figure 29 resulted from the wide variation in excitation frequencies, which resulted in different amounts of amplification. The effect of excitation frequency on amplification factors is shown in figure 30.

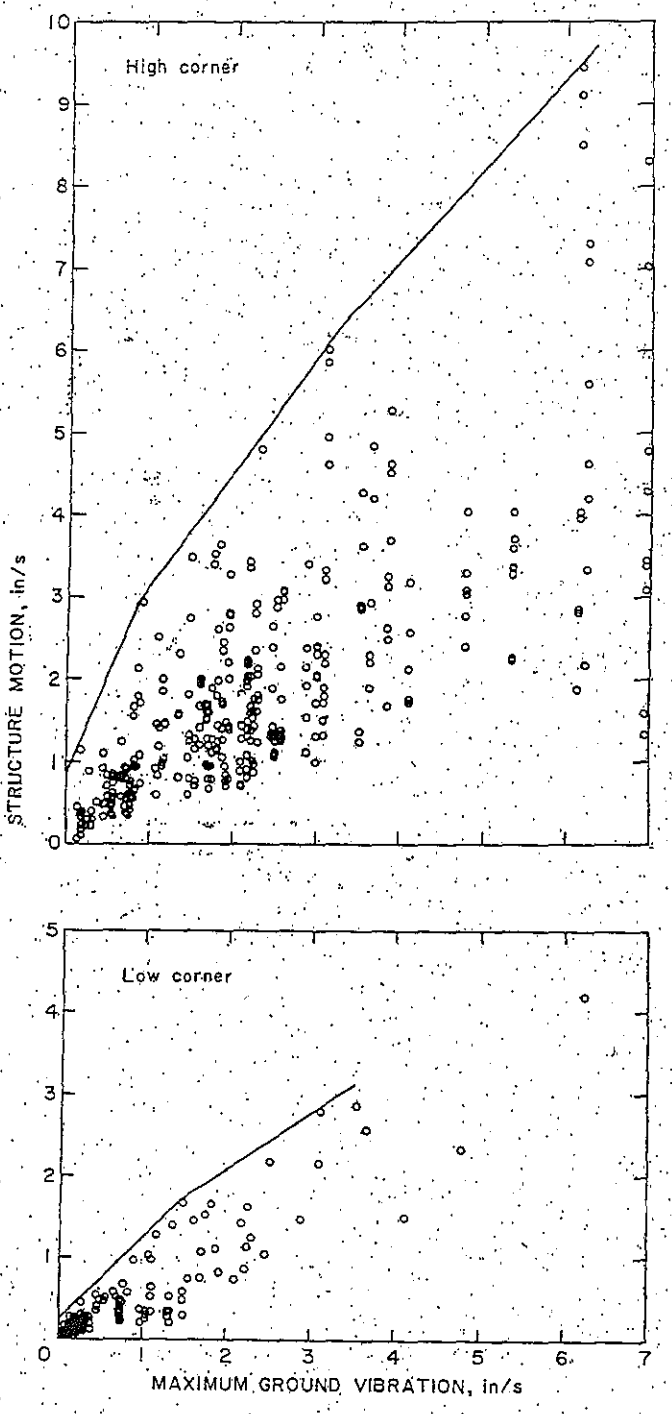

FIGURE 29. - Low- and high-corner responses versus maximum ground vibration.

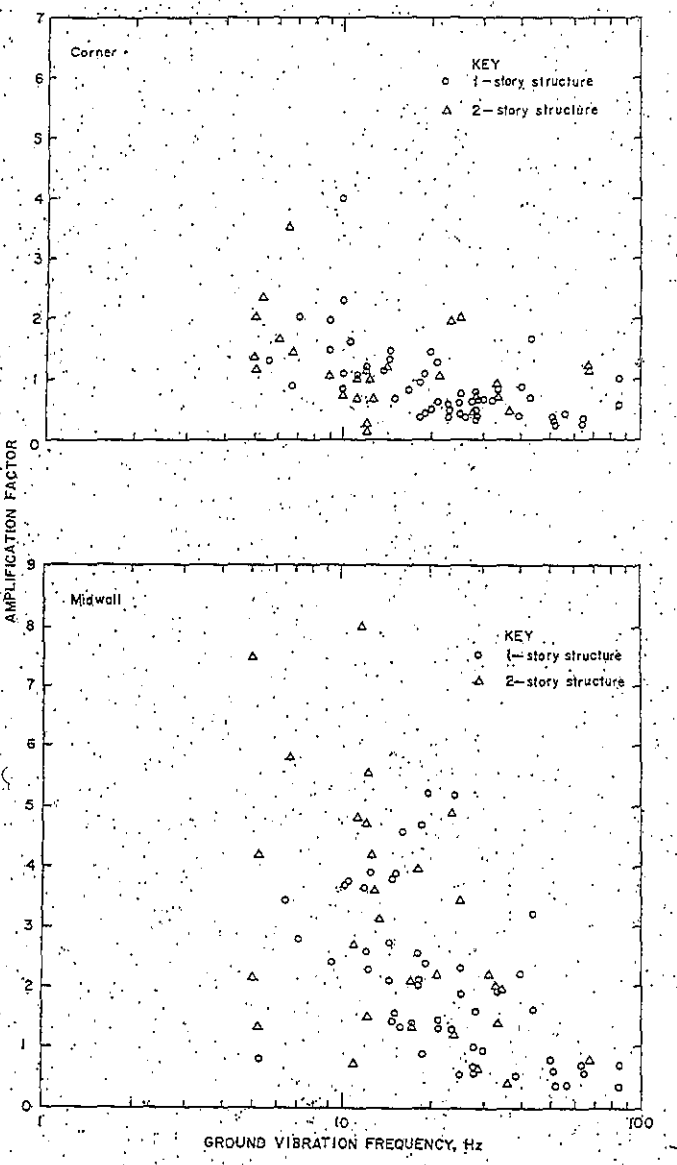

FIGURE 30. - Corner and midwall amplification factors (2).

Strains in walls from airblast are shown in figure 31. Based on the worst-case envelopes of airblast and ground vibration versus strain, an airblast of ~ 132 dB produces the same wall strains as a ground vibration of 1 in/s. This equality applies only to airblasts whose peak amplitudes occur at frequencies within the range of the frequencies of the structure's midwalls. Otherwise, typical airblasts in these tests induced strains of less than 25 μin/in, even for airblasts approaching 132 dB. The measured strains were equivalent to those produced by a ground vibration of 0.25 in/s. In the time histories, the maximum strain responses usually coincided with the arrival of frequencies near the structure's natural frequency. Figure 31 also includes the induced strains recorded in one of the houses in the previously discussed sonic-boom study (3). The larger structure response from the mine blasts is the result of a better match of the frequency content of the confined blasts to the natural frequency of the wall panels.

As illustrated in figure 32, strain response is a combination of both shear and flexural deformation of the walls. Plots of strain versus maximum ground vibration are shown for wallboard and plaster, wallboard tape joints, block joints, and brick veneer, and fireplace brick joints in figures 33-37, respectively. The graph of peak wallboard and plaster strain (fig. 33) shows a large scatter of data again (as in figure 29) due to differences in excitation frequency and mode at the same maximum vibration level, or peak particle velocity. Wallboard and taped joints were exposed to maximum strains of 250 to 550 μin/in, which is considerably below the 1,000 μin/in necessary for visible cracking. However, these are dynamic strains, and they do not include prestrains. Since no cracks were observed in the wallboard, the prestrains were probably less than 500 μin/in.

Wallboard crack resistance is influenced by flexibility in end constraints such as nails. These end constraints do not efficiently transfer vibration energy from the superstructure to the wallboard. Accordingly, it was observed that cracks developed primarily in the plastered joints at wall corners and in plaster coverings over nailheads.

The strain level at first cracking of masonry walls is 770 to 7,700 μin/in using a visual displacement range of 0.01 to 0.10 mm for joints 13 mm wide. For site strains observed at the test house to reach the 3,270-μin/in level observed by Crawford during a blast (31), particle velocities would have to exceed 0.75 in/s. It is not known whether a strain or displacement criterion should be used for the propagation of step-like cracks across a wall, but research planned for 1984 by the National Bureau of Standards should provide additional insights.

SHAKER-INDUCED RESPONSE

The shaker program began immediately upon completion of the blasting work. Because of time constraints and the superstructure's resistance to low-level blast vibrations, plans were to operate the shakers at levels that would produce a structure response equivalent to the response caused by ground vibrations of 0.5 to 2.0 in/s. The response of the transducer at location A_4, high corner, east wall, was used to set shaker force. (See figures 13 and 28.) Strain levels and the number of cycles to cracking were of primary interest, so each test was run until cracking was observed or ~ 100,000 cycles was reached. The house was shaken at a constant amplitude with a frequency sweep from 2 to 12 Hz before and after each test to find any changes in dynamic properties of natural frequency and damping.